Tetrahedral Complexes Containing the $Fe^{II}S_4$ Core. The Syntheses, Ground-State Electronic Structures, and Crystal and Molecular Structures of the $[P(C_6H_5)_4]_2Fe(SC_6H_5)_4$ and $[P(C_6H_5)_4]_2Fe(S_2C_4O_2)_2$ Complexes. An Analogue for the Active Site in Reduced Rubredoxins (Rd_{red})

D. Coucouvanis,* D. Swenson, N. C. Baenziger, C. Murphy, D. G. Holah, N. Sfarnas, A. Simopoulos, and A. Kostikas

Contribution from the Department of Chemistry, University of Iowa, Iowa City, Iowa 52242, and the Nuclear Research Center, "Demokritos", Aghia Paraskevi, Attiki, Greece.
Received April 29, 1980

Abstract: The synthesis of the $[P(C_6H_5)_4]_2Fe(SC_6H_5)_4$ (I) and $[P(C_6H_5)_4]_2Fe(S_2C_4O_2)_2$ (II) complexes is described in detail. I crystallizes in the orthorhombic, polar space group $Pbc2_1$, with four molecules in the unit cell. The cell dimensions are a = 13.797 (3) Å, b = 17.542 (4) Å, and c = 24.913 (5) Å. II crystallizes in the monoclinic space group $P2_1/c$ with four molecules in the unit cell. The cell dimensions are a = 17.402 (7) Å, b = 16.680 (5) Å, c = 18.242 (6) Å, and β = 110.53 (2)°. Intensity data for both I and II were collected with a four-circle computer-controlled diffractometer with use of the θ–2θ scan technique. In both structures the carbon atoms in the cations were refined with isotropic temperature factors. In both structures all other nonhydrogen atoms were refined with anisotropic temperature factors. Refinement by full-matrix least squares of 472 parameters on 4929 data for I and 308 parameters on 2801 data for II gave final R values of 0.047 and 0.055 for I and II, respectively. In both structures the hydrogen atoms were included in the structure factor calculation but were not refined. The overall description of the FeS_4 central unit in both I and II is that of a distorted tetrahedron formed by four monodentate $SC_6H_5^-$ ligands in I and two bidentate $S_2C_4O_2^{2-}$ chelates in II. Average values of selected structural parameters and the standard deviations of the mean for the two structures are as follows. For I: Fe–S = 2.353 (9) Å; S–S = 3.837 (18) Å; C–S = 1.767 (19) Å; Fe–S–C = 110.8 (1.9)°; range in S_i–Fe–S_j angles = 97.89 (9)–119.00 (10)°. For II, Fe–S = 2.389 (7) Å; S–S(bite) = 3.922 (14) Å; C–S = 1.688 (9) Å; Fe–S–C = 92.1 (8)°; range in S_i–Fe–S_j angles = 95.57 (11)–124.86 (13)°. The distortions in the FeS_4 tetrahedron in II arise from steric constraints from the $S_2C_4O_2^{2-}$ ligand. A complete analysis of various structural parameters in a number of $[M(SC_6H_5)_4]^{2-}$ tetrahedra with M = Ni, Co, Zn, Cd, and Fe and for two different types of counterions reveals that the distortions of the MS_4 central unit arise from intramolecular, ortho phenyl hydrogen–sulfur and metal interactions. The Mössbauer spectra of I and II have been studied as a function of temperature and an externally applied magnetic field. Values of the fine and hyperfine parameters for I and the magnetic moment (μ_{eff} = 5.1 μ_B) are very similar to those reported for reduced rubredoxin (Rd_{red}). The visible spectra of I also are similar to those obtained for Rd_{red}. On the basis of the available data it is clear that the electronic ground state for I is very similar to the one in Rd_{red}.

At the time that our studies on the coordination chemistry of monomeric mercaptide complexes were initiated, the only structurally characterized examples of such species that were reported, occurred as $M(S\text{-}Cys)_4$ centers in certain metalloenzymes. The presence of $[M(S\text{-}Cys)_4]$ tetrahedral sites has been established by crystallographic studies in oxidized rubredoxin (Rd_{ox}) from *Clostridium pasteurianum*[1] (M = Fe(III)) and in horse liver alcohol dehydrogenase, LADH, (M = Zn(II)).[2] Indirectly, the $[Co(S\text{-}Cys)_4]$ chromophore was detected in the characteristic ligand field spectrum of Co(II)-substituted LADH.[3]

Rubredoxins, the simplest of the nonheme iron sulfur redox proteins, have molecular weights that are typically about 6000 daltons and are obtained from bacteria.[4-6] A common feature among all these proteins is one $[Fe(S\text{-}Cys)_4]$ active site and in the case of Rd from pseudomonas oleovarans (mol wt ~19000) two such sites which apparently are noninteracting.[7]

Extensive investigations of the $[Fe(S\text{-}Cys)_4]$ active centers in the rubredoxins have been conducted by magnetic susceptibility,[8] optical absorption,[4a,9,10] MCD,[4a,11] EPR,[12] and Mössbauer spectroscopy.[8,12,13] These studies have shown that the two redox states of the proteins, Rd_{ox} and Rd_{red}, contain tetrahedrally coordinated Fe(III) and Fe(II), respectively. Electrochemical studies show the Fe(III)–Fe(II) couple at a potential (E_0') that varies from −0.04 to −0.06 v.[14] The X-ray structure determination of *Clostridium pasteurianum* Rd_{ox} at 1.5-Å resolution[1] shows a severely distorted $[Fe^{III}(S\text{-}Cys)_4]$ tetrahedral site with one of the Fe–S bonds unusually short (2.05 Å). Two other structural studies of the active site in Rd_{ox} by X-ray absorption fine structure (EXAFS) analyses have been reported. In lyophilized *P. aerogenes* Rd_{ox}[15] and in *C. pasteurianum* Rd_{ox},[16] these analyses have led to

* Address correspondence to D.C. at the University of Iowa: D.C., D.S., N.C.B., C.M., and D.G.H—University of Iowa; N.S., A.S., and A.K.—Nuclear Research Center.

(1) (a) Watenpaugh, K. D.; Sieker, L. C.; Herriott, J. R.; Jensen, L. H. *Acta Crystallogr., Sect. B* **1973**, *B29*, 943. (b) Jensen, L. H. In "Iron-Sulfur Proteins"; Lovenberg, W., Ed.; Academic Press: New York, 1973; Vol. II, Chapter 4.
(2) Eklund, H.; Nordström, B.; Zeppezauer, E.; Söderlund, G.; Ohlesson, I.; Boiwe, T.; Bränden, C. I. *FEBS Lett.* **1974**, *44*, 200. Eklund, H.; Nordström, B.; Zeppezauer, E.; Söderlund, E.; Ohlesson, I.; Boiwe, T.; Soderberg, B. O.; Tapia, O.; Bränden, C. I. *J. Mol. Biol.* **1976**, *102*, 27.
(3) Drum, D. E.; Valee, B. L. *Biochem. Biophys. Res. Commun.* **1970**, *41*, 33.
(4) (a) Eaton, W. A.; Lovenberg, W. In "Iron-Sulfur Proteins"; Lovenberg, W., Ed.; Academic Press: New York, 1973; Vol. II, Chapter 3. (b) Lovenberg, W. In "Microbial Iron Metabolism"; Neilands, J. B., Ed.; Academic Press: New York, 1974; Chapter 8.
(5) Jensen, L. H. *Annu. Rev. Biochem.* **1974**, *43*, 461.
(6) Orme-Johnson, W. H. *Annu. Rev. Biochem.* **1973**, *42*, 159. Palmer, G. In "The Enzymes", Part B, 3rd ed.; Boyer, P. D., Ed.; Academic Press: New York, 1975; Vol. XII, Chapter 1.
(7) Lode, T.; Coon, M. J. *J. Biol. Chem.* **1971**, *246*, 791.
(8) Phillips, W. D.; Poe, M.; Weiher, J. F.; McDonald, C. C.; Lovenberg, W. *Nature (London)* **1970**, *227*, 574.
(9) Lovenberg, W.; Williams, W. M. *Biochemistry* **1969**, *8*, 141.
(10) Eaton, W. A.; Palmer, G.; Fee, J. A.; Kimura, T.; Lovenberg, W. *Proc. Natl. Acad. Sci. U.S.A.* **1971**, *68*, 3015.
(11) Ulmer, D. D.; Holmquist, B.; Vallee, B. L. *Biochem. Biophys. Res. Commun.* **1973**, *51*, 1054.
(12) Cammack, R.; Dickson, D. P. E.; Johnson, C. E. In "Iron-Sulfur Proteins"; Lovenberg, W., Ed.; Academic Press: New York, 1977; Vol. III, Chapter 8 and references therein.
(13) Debrunner, P. G.; Münck, E.; Que, L.; Schulz, C. E. In "Iron-Sulfur Proteins"; Lovenberg, W., Ed.; Academic Press: New York, 1977; Vol. III, Chapter 10 and references therein.
(14) (a) Peterson, J. A.; Coon, M. J. *J. Biol. Chem.* **1968**, *243*, 329. (b) Lovenberg, W.; Sobel, B. E. *Proc. Natl. Acad. Sci. U.S.A.* **1965**, *54*, 193.
(15) Shulman, R. G.; Eisenberger, P.; Blumberg, W. E.; Stombaugh, N. A. *Proc. Natl. Acad. Sci. U.S.A.* **1975**, *72*, 4003.

0002-7863/81/1503-3350$01.25/0

the conclusion that the Fe–S distances in the Fe^{III}–S_4 centers are closer to being equal than the results from the crystallographic studies indicate.[1]

Monomeric, tetrahedral FeS_4 complexes with simple ligands are few. A survey of the literature shows the following molecules that can be considered as models at various levels of characterization and significance: $Fe[(SPR_2)_2N]_2$,[17a] $Fe[(SPR_2)_2CH]_2$,[17b] $[Fe(12\text{-peptide})]^{2-}$,[18] $[Fe(S_2\text{-}o\text{-xyl})_2]^{2-}$ (xyl = xylene), and $[Fe(S_2\text{-}o\text{-xyl})_2]^-$.[19] The last two entries in this list of complexes represent to date the most successful analogues for Rd_{red} and Rd_{ox} to the extent that, in addition of being structural analogues, they display both oxidation levels, Fe^{II}/–S_4 and Fe^{III}–S_4, found in Rd_{red} and Rd_{ox}, respectively.[19]

With the exception of the $[Fe(S_2\text{-}o\text{-xyl})_2]^{2-}$ complex none of the other Fe^{II}–S_4 complexes, including the ones reported in this paper, seem to afford stable Fe^{III}–S_4 complexes upon oxidation.

In our attempts toward the synthesis of tetrahedral complexes with the MS_4 central unit, we were successful in obtaining a series of such complexes with the new dithiosquarate $(S_2C_4O_2)^{2-}$ ligand.[20,21]

This ligand, under considerable strain while coordinated, proved to be a useful leaving group in metatheses reactions. One such general reaction with the thiophenolate anion $(SC_6H_5)^-$ was utilized for the synthesis of two new series of tetrahedral MS_4 complexes.[22] The "mixed" ligand $[M(S_2C_4O_2)(SC_6H_5)_2]^{2-}$, X-ray isomorphous, complexes (M = Mn, Fe, Co, Zn) were found to be high-spin, tetrahedral anions. The $[M(SC_6H_5)_4]^{2-}$ complexes (M = Mn, Fe, Co, Ni, Zn, Cd) also were found high-spin, tetrahedral anions, and their structures have been determined.[23]

Mössbauer studies on the $[Fe(SC_6H_5)_4]^{2-}$ (I), $[Fe(S_2C_4O_2)_2]^{2-}$ (II), and $[Fe(S_2C_4O_4)(SC_6H_5)_2]^{2-}$ (III) complexes have revealed a great similarity between the spectra of I and those of reduced rubredoxin.[24] In this paper we report on the detailed molecular and electronic structures of the tetraphenylphosphonium, $[PPh_4]^+$, salts of I and II.

Experimental Section

Synthetic Procedures. The syntheses of all complexes were performed under a pure dinitrogen atmosphere in a vacuum atmosphere Dri-lab glovebox. Potassium dithiosquarate, $K_2S_2C_4O_2$, was prepared as described previously.[20] Acetonitrile was purified by distillation from calcium hydride and stored over molecular sieves. Diethyl ether was purified by distillation after standing over sodium wire for ca. 24 h. $[Ph_4P]_2[Fe(S_2C_4O_2)_2]$[20] and $[Et_4N]Fe[EtXant]_3$[25] were synthesized as described previously. KSC_6H_5 was obtained by the reaction between potassium metal and thiophenol in tetrahydrofuran.

Bis(tetraphenylphosphonium) Tetrakis(thiophenolato)ferrate(II), $[Ph_4P]_2[Fe(SC_6H_5)_4]$. (a) To a solution of 4.4 g $[Et_4N]Fe(EtXant)_3$ (EtXant = O-ethyldithiocarbonate) (0.8 mmol) in 30 mL of acetonitrile was suspended 4.4 g of KSC_6H_5 (4.0 mmol), and the suspension was boiled for ca. 5 min. At this state 5.9 g of Ph_4PCl (1.6 mmol) was added and heating continued for an additional 10 min. The mixture was filtered while hot to remove unreacted KSC_6H_5 and the KEtXant and KCl byproducts. When the solution was left standing, large light red brown crystals formed which were isolated, washed with diethyl ether, and dried. A 3.5-g sample of the product (37%) was obtained. Addition of ether (20 mL) to the filtrate resulted in the formation of more of the crystalline product, 4.1 g, for an overall yield of 81%. Anal. Calcd for $C_{72}H_{60}P_2FeS_4$: C, 73.76; H, 5.16; Fe, 4.77; S, 10.93; fw, 1171.29. Found: C, 73.70; H, 5.07; Fe, 4.75; S, 10.55.

(b) The same synthetic procedure as above was followed, using $[Ph_4P]_2Fe(S_2C_4O_2)_2$ instead of $[Et_4N]Fe(EtXant)_3$ and eliminating the addition of Ph_4PCl. The $[Ph_4P]_2Fe(SC_6H_5)_4$ product was obtained in 85% yield.

(c) **Bis(tetraethylammonium) Tetrakis(thiophenolato)ferrate(II), $[Et_4N]_2Fe[(SC_6H_5)_4]$.** To a solution of 4.0 g of $[Et_4N]Fe(EtXant)_3$ (0.73 mmol) and 0.97 g of Et_4NCl (0.6 mmol) in 20 mL of CH_3CN was added 4.0 g of KSC_6H_5 (3.67 mmol), and the suspension was brought to the boiling point of acetonitrile. After 15 min of boiling the hot suspension was filtered. A 10-mL sample of absolute EtOH was added to the filtrate, and diethyl ether was added slowly until the first permanent cloudiness appeared in solution. When the solution was left standing for ca. 0.5 h, brown-red needle like crystals of the product formed and were isolated (3.2 g, 58% yield). Anal. Calcd for $C_{40}H_{60}N_2FeS_4$: C, 63.74; H, 7.97; S, 17.03; Fe, 7.38; fw, 753.00. Found: C, 63.55; H, 7.85; S, 17.00; Fe, 7.25.

Physical Measurements. Mössbauer spectra were measured from 1.1 K to room temperature with a constant acceleration spectrometer. The source was 100 of mCi ^{57}Co in Rh matrix and held at room temperature. Measurements were also made with the absorber in external magnetic fields up to 65 kOe with a superconducting magnet operating in a transverse configuration. Magnetic susceptibility measurements were carried out with a vibrating sample magnetometer from 4.2 K to room temperature. Reflectance spectra were recorded with a DK-2 Spectrometer and solution spectra with a Cary Model 14 spectrophotometer.

X-ray Diffraction Measurements. Collection and Reduction of Data. Specific details concerning crystal characteristics and X-ray diffraction methodology are shown in Table I. The crystals of both compounds were mounted on a Picker-Nuclear four-circle diffractometer automated by a DEC-PDP8-I computer with FACS-I DOS software and equipped with a molybdenum-target X-ray tube, a graphite-monochromator ($2\theta_{max}$ = 12.20°) crystal detector, and pulse-height analyzer. All measurements were made at ambient temperature (ca. 24 °C). For both structures 12 reflections with 2θ values between 20 and 30° (Mo K$\bar{\alpha}$, λ = 0.7107 Å) were centered on the diffractometer, and the preliminary cell dimensions were refined on the 2θ values of these reflections to yield the cell parameters shown in Table I. The diffraction peaks were measured by using a stepped θ–2θ scan data collection technique.[26] The least-squares procedure used minimized the function $\sum w(|F_o| - |F_c|)^2$, and we assigned $w = 0.0$ if $F^2 < 3\sigma(F^2)$. The atomic scattering factors of the neutral

Table I. Crystal and Refinement Data

	I	II
formula	$[P(C_6H_5)_4]_2[Fe(SC_6H_5)_4$	$[P(C_6H_5)_4]_2$-$[Fe(S_2C_4O_2)_2]$
mol wt	1171.29	1023.00
cell dimens		
a, Å	13.797 (3)	17.402 (7)
b, Å	17.542 (4)	16.680 (5)
c, Å	24.913 (5)	18.242 (6)
β, deg		110.53 (2)
V, Å^3	6029.6	4958.7
Z	4	4
d_{calcd}, g/cm^3	1.290	1.374
d_{obsd},[a] g/cm^3	1.29 (1)	1.38 (1)
space group	$Pbc2_1$	$P2_1/c$
cryst dimens, mm	0.5 × 0.5 × 0.6	0.1 × 0.3 × 0.2
μ, cm^{-1}	4.88	5.82
radiatn	Mo (λ = 0.7107 Å); monochromatized from a pyrolytic graphite crystal, $2\theta_{max}$ = 12.2°	
2θ limit, deg	45	40
unique reflctns	5672	4624
reflctns used, $F^2 > 3\sigma(F^2)$	4929	2801
function minimized	$\Sigma w(F_o^2 - F_c^2)^2$	
w	$1/\sigma^2(F_o^2)$	
variable parameters	472	308
R_1[b]	0.047	0.055
R_2[c]	0.059	0.066

[a] Determined by flotation in a CCl_4-pentane mixture. [b] $R_1 = \Sigma|\Delta F|/\Sigma|F_o|$. [b] $R_2 = [\Sigma w(\Delta F)^2/\Sigma w|F_o|^2]^{1/2}$.

(16) Sayers, D. E.; Stern, E. A.; Herriott, J. R. *J. Chem. Phys.* **1976**, *64*, 427.
(17) (a) Davison, A.; Switkes, E. S. *Inorg. Chem.* **1971**, *10*, 837. (b) Davison, A.; Reger, D. L. *Ibid.* **1971**, *10*, 1967.
(18) Anglin, J. R.; Davison, A. *Inorg. Chem.* **1975**, *14*, 234.
(19) Lane, R. W.; Ibers, J. A.; Frankel, R. B.; Papaefthymiou, G. C.; Holm, R. H. *J. Am. Chem. Soc.* **1977**, *99*, 84.
(20) (a) Coucouvanis, D.; Holah, D. G.; Hollander, F. J. *Inorg. Chem.* **1975**, *14*, 2657. (b) Hollander, F. J.; Coucouvanis, D. *J. Am. Chem. Soc.* **1977**, *99*, 6268.
(21) Coucouvanis, D.; Swenson, D.; Baenziger, N. C.; Holah, D. G.; Kostikas, A.; Simopoulos, A.; Petrouleas, V. *J. Am. Chem. Soc.* **1976**, *98*, 5721.
(22) Holah, D. G.; Coucouvanis, D. *J. Am. Chem. Soc.* **1975**, *97*, 6917.
(23) Swenson, D.; Baenziger, N. C.; Coucouvanis, D. *J. Am. Chem. Soc.* **1978**, *100*, 1932. Swenson, D. Ph.D. Thesis, University of Iowa, 1979.
(24) Kostikas, A.; Petrouleas, V.; Simopoulos, A.; Coucouvanis, D.; Holah, D. G. *Chem. Phys. Lett.* **1976**, *38*, 582.
(25) Holah, D. G.; Murphy, C. N. *Can. J. Chem.* **1971**, *16*, 2726.
(26) Baenziger, N. C.; Foster, B. A.; Howells, M.; Howells, R.; Vander Valk, P.; Burton, D. J. *Acta Crystallogr., Sect. B* **1977**, *B33*, 2327.

atoms were used,[27] and all the scattering factors except those for hydrogen[28] were corrected by adding real and imaginary terms to account for the effects of anomalous dispersion.[29]

(I) $[(C_6H_5)_4P]_2[Fe(SC_6H_5)_4]$. A fresh crystal was lodged in a glass capillary for data collection. Three "standard" reflections were measured after every 50 data points to monitor crystal and instrumental stability. No systematic change over the data collection period was observed. Data were collected in the full sphere of the reciprocal space out to a 2θ value of 45°. The systematic absences $0kl$, $k = 2n + 1$, $h0l$, $l = 2n + 1$, indicated either the centrosymmetric space group *Pbcm* or the noncentrosymmetric space group $Pbc2_1$. Lorentz–polarization corrections were made, and no absorption corrections were applied to the data.

(II) $[(C_6H_5)_4P]_2[Fe(S_2C_4O_2)_2]$. A crystal was mounted in a glass capillary and used for cell dimension measurement and data collection. Data were collected as previously described for I. All data in the hemisphere of reciprocal space $h,\pm k,\pm l$ were collected to a 2θ angle of 40°. The systematic absences $0k0$, $k \neq 2n$, and $h0l$, $l \neq 2n$, establish the centrosymmetric space group $P2_1/c$. The data were corrected for Lorentz and polarization effects as described for I.

Determinations of the Structures. (I) $[(C_6H_5)_4P]_2[Fe(SC_6H_5)_4]$. The structure determination initially was carried out by using a limited data set ($2\theta_{max} = 30°$, Mo Kα, 1435 unique reflections). The distribution of normalized intensities gave no indication of the actual space group; hence *Pbcm* was chosen for convenience. The Patterson map yielded the coordinates of the Fe atom and S atoms with the Fe atom and two S atoms positioned on a mirror plane. Successive electron density maps yielded no more information until the space group was reduced to $Pbc2_1$.[30] The rest of the molecule was then slowly revealed and, on the basis of the 999 reflections with $F^2 > 3\sigma(F^2)$ was refined by using a block-diagonal least-squares program[31] to an R_1 value of 0.10. At this point the temperature factors of the Fe, S, and P atoms were refined anisotropically with the phenyl rings treated as rigid groups[32] (C–C and C–H bond lengths set at 1.390 and 0.95 Å, respectively; individual isotropic temperature factors for the C atoms; H temperature factors set equal to the temperature factor of the C atom to which each is bonded). Refinement by a full-matrix least-squares computer program[33] reduced the R value to 0.042. At this stage we reported on the results in a communication.[21] The somewhat large standard deviations (0.006 Å for the Fe–S bond lengths) prompted us to obtain a new data set on a larger crystal to $2\theta_{max} = 45°$. Of the 5672 unique reflections thus obtained, 4929 had $F^2 > 3\sigma(F^2)$ and were used in the least-squares refinement. The refinement of all individual nonhydrogen atoms of the anion with anisotropic temperature factors and of the individual nonhydrogen atoms in the cations with isotropic temperature factors converged to R_1 and R_2 values of 0.0475 and 0.0592, respectively. In this refinement the hydrogen atoms were included in the structure factor calculation at their calculated positions but were not refined. With the second data set smaller standard deviations in the interatomic distances and angles were obtained (Table IV). Because of the fact that the $Pbc2_1$ is a polar space group, the absolute configuration of a particular crystal must be established. The final refinements on all members of the series of the X-ray isomorphous $[Ph_4P]_2[M(SPh_4)]_4$ complexes were made for both enantiomers. The results for the iron member of the series are typical. For the correct choice of the enantiomer $R_1 = 0.0475$ and $R_2 = 0.0592$ compared to $R_1 = 0.0541$ and $R_2 = 0.0696$ for the other choice. The Fe–S distances and bond angles do not differ significantly between the two choices of enantiomers. Averaging Friedel pairs and fitting to the wrong enantiomer gave $R_1 = 0.0470$ and $R_2 = 0.0590$; two Fe–S bond distances were not significantly different from the correct enantiomer choice, and the scatter of Fe–S distances was greater.

(II) $[Fe(S_2C_4O_2)_2]^{2-}[Ph_4P]_2^+$. From the intensity data (Table I) a set of structure factors was obtained which was used to compute a three-dimensional Patterson map. The iron and four sulfur atom positions were determined from this map. An electron density map phased on the input positions of these five atoms revealed the positions of the two independent phosphorus atoms and the rest of the atoms in the $Fe(S_2C_4O_2)_2^{2-}$ anion. Subsequent electron density maps showed the positions of all the remaining carbon atoms of the Ph_4P cations. Isotropic refinement of all nonhydrogen atoms resulted in a R value of 0.11. The complex anion

(27) Doyle, P. A.; Turner, P. S. *Acta Crystallogr., Sect. A* **1968**, *A24*, 390.
(28) Stewart, R. F.; Davidson, E. R.; Simpson, W. T. *J. Chem. Phys.* **1965**, *42*, 3175.
(29) Cromer, D. T.; Liberman, D. *J. Chem. Phys.* **1970**, *53*, 1891.
(30) The equipoints for the nonstandard $Pbc2_1$: $x, y, z; -x, \frac{1}{2} + y, z; -x, -y, \frac{1}{2} + z; x, \frac{1}{2} - y, \frac{1}{2} + z$.
(31) BDLA: Baenziger, N. C., locally written computer program.
(32) Scheringer, C. *Acta Crystallogr.* **1963**, *16*, 546.
(33) LESQUI: Lawrence Berkeley Laboratory, full-matrix least-squares computer program, modified for local use by F. J. Hollander.

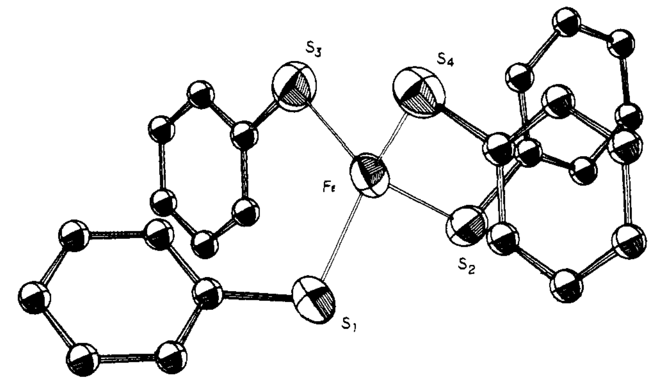

Figure 1. Structure and labeling of the $Fe(SC_6H_5)_4^{2-}$ anion. Thermal ellipsoids as drawn by ORTEP (Johnson, C. K. ORNL-3794; Oak Ridge National Laboratory: Oak Ridge, TN, 1965) represent the 50% probability surfaces.

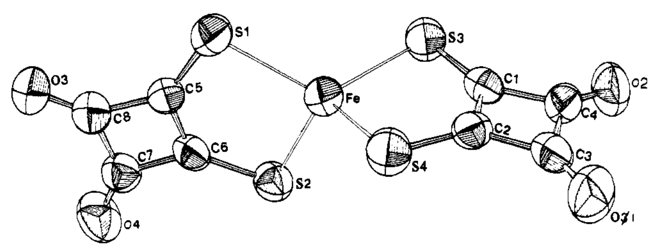

Figure 2. Structure and labeling of the $Fe(S_2C_4O_2)_2^{2-}$ anion. Thermal ellipsoids represent the 50% probability surfaces.

and the two phosphorus atoms were then refined with anisotropic thermal parameters, keeping isotropic thermal parameters for the cation carbon atoms. This refinement converged to a value for R of 0.071. At this stage a difference Fourier revealed the presence of several of the hydrogen atoms in the cations. The positions of all 40 hydrogens were calculated (C–H at 0.95 Å) and included in the structure factor calculation but not refined, with temperature factors equal to the mean temperature factor of the carbon atoms in the corresponding phenyl rings on which the H atoms were attached. The final values for R_1 and R_2 were 0.055 and 0.066, respectively. In the final difference Fourier map no peaks higher than ~0.3 e A^3 were found.

Crystallographic Results. The final atomic positional and thermal parameters for I with standard deviations derived from the inverse matrix of the last least-squares refinement are compiled in Table II. The corresponding data for II are tabulated in Table III.

Intramolecular distances and angles for I are given in Table IV. Corresponding results for I are presented in Table V. The atom-labeling schemes are shown in Figures 1 and 2. Stereoviews are shown in Figures 3 and 4.

The generated atomic parameters of the hydrogen atoms have been deposited together with a table of the observed values of F, their esd's, and the $|F_o| - |F_c|$ values. (See paragraph at the end of the paper regarding supplementary material.)

Results and Discussion

Structural Descriptions. (I) $[Ph_4P]_2[Fe(SC_6H_5)_4]$. The packing of the anions and cations in the unit cell grossly resembles the ZnS lattice. The four anions are found in an approximate tetrahedral arrangement around $x = \frac{1}{2}$, $y = \frac{3}{4}$, and $z = \frac{1}{4}$, with the central metal atoms lying on approximate mirror planes at $z = \frac{1}{2}$ and $z = 0$. The eight tetraphenylphosphonium cations pack above and below the anions at $z \approx \frac{1}{4}$ and $\frac{3}{4}$. As the unit cell contents arrangement indicates (Figure 4), the crystal structure is an open structure with no indication of unusual crowding that would be necessary to cause distortions in either the cations or the anions. There are only three carbon–carbon or carbon–hydrogen atom distances less than van der Waals contacts (van der Waals radii for H equals 1.20 Å and 1.57 Å[34,35] between the anions and cations.

(34) Pauling, L. "The Nature of the Chemical Bond", 3rd ed.; Cornell University Press: Ithaca, NY, 1960.
(35) Purcell, K. F.; Kotz, J. C. "Inorganic Chemistry"; W. B. Saunders: Philadelphia, 1977.

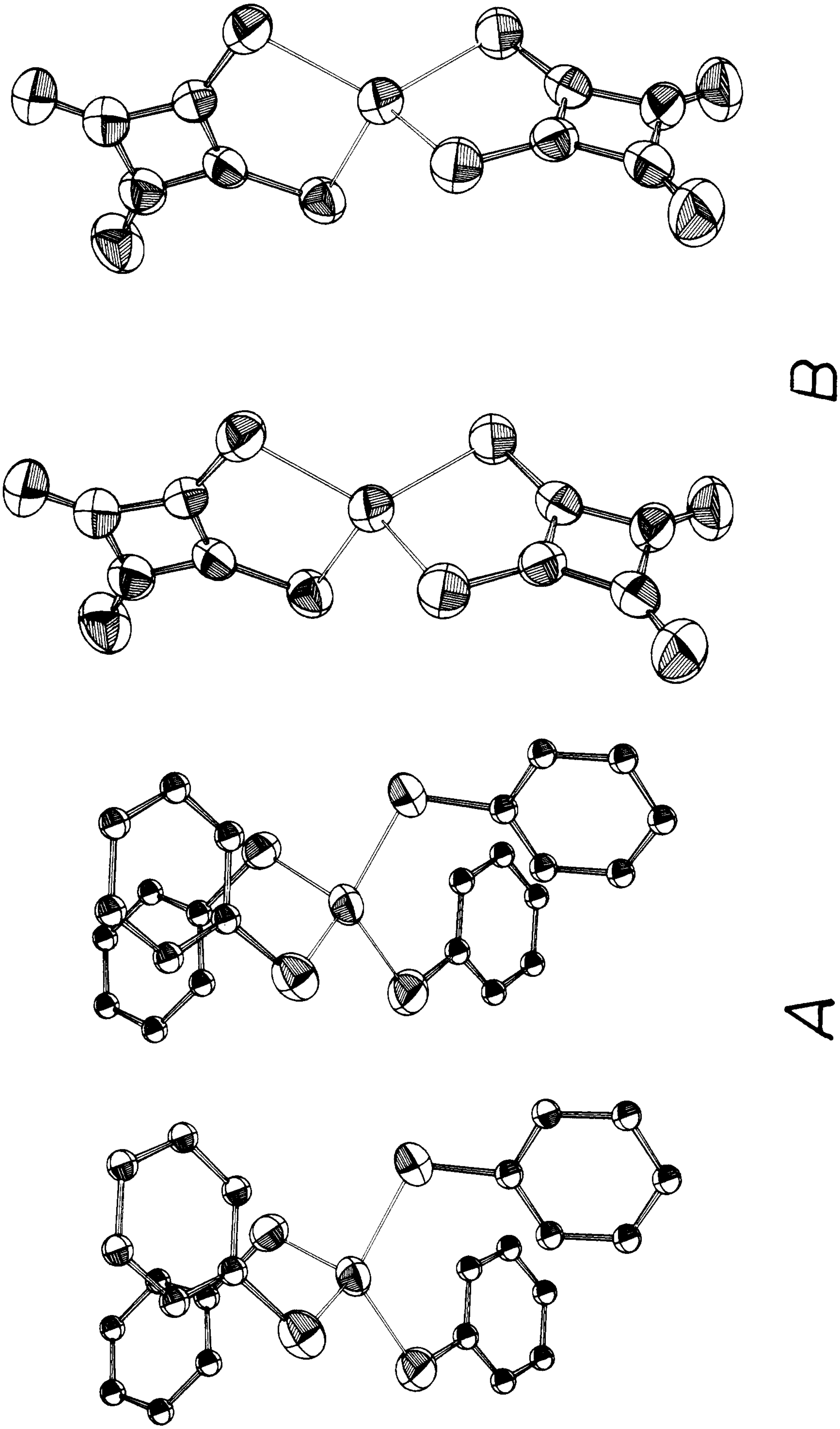

Figure 3. Stereoscopic views of (A) $Fe(SC_6H_5)_4^{2-}$ and (B) $Fe(S_2C_4O_2)_2^{2-}$ as drawn by ORTEP.

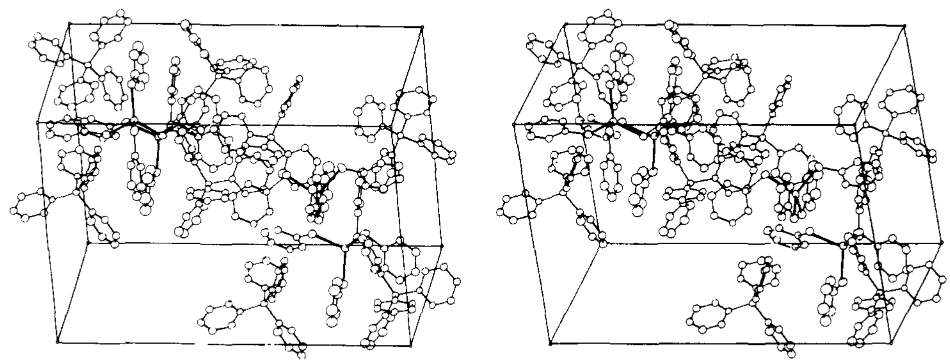

Figure 4. Unit cell contents of $[(C_6H_5)_4P]_2Fe(SC_6H_5)_4$.

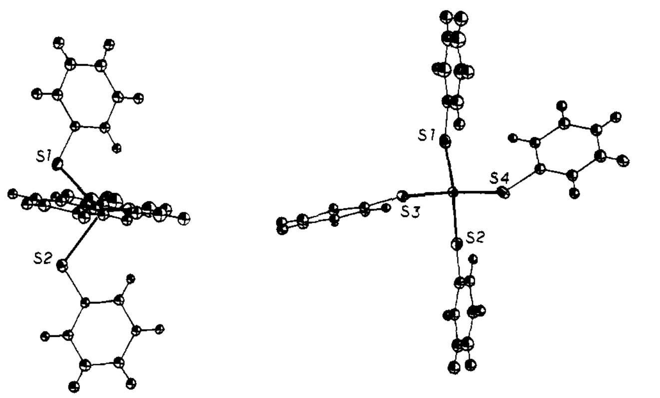

Figure 5. Two views of the $Fe(SC_6H_5)_4^{2-}$ anion where the particular disposition of the phenyl rings is apparent. A rotation of the phenyl ring on S_4 by ca. 15° out of the S_3FeS_4 plane apparently is a result of crystal packing effects.

However, while no distortions are apparent in the structure of the tetrahedral Ph_4P^+ cations, severe distortions from tetrahedral geometry are observed in the structure of the $[Fe(SC_6H_5)_4]^{2-}$ anion (I). In the Fe^{II}–S_4 unit the Fe–S distances range from 2.338 (2) to 2.360 (2) Å with a mean value of 2.353 (9) Å,[36] a value similar to those reported for the Fe–S bonds in the $[Fe(S_2\text{-}o\text{-xyl})_2]^{2-}$[19] and $Fe[(SPMe_2)_2N]_2$[17a] complexes of 2.356 (22) and 2.360 (9) Å, respectively. The range and mean values of the S–Fe–S angles in I are 97.89 (9)–119.00 (10)° and 109.6 (7.6)°, respectively. The corresponding values of 103.5 (2)–114.9 (2)° and 109.5° reported for the structure of the $[Fe(S_2\text{-}o\text{-xyl})_2]^{2-}$ anion show that the former is subject to considerably greater angular distortions from T_d symmetry than the latter. The distortions in I can be envisioned, grossly, as a compression of the FeS_4 tetrahedron along one of its twofold axes.

In the initial communication of the structure of I the angular distortions were attributed[21] to a possible manifestation of the Jahn–Teller affect (^5E, T_d ground state). The validity of this suggestion was explored by structure determinations[23] of other $[M(SC_6H_5)_4]^{2-}$ complexes (M = Ni, Mn, Co, Zn, Cd). Similar distortions of the MS_4 units were found even with metal ions with nondegenerate ground states, and it became apparent that the Jahn–Teller effect was not the *only* reason for the distorted FeS_4 unit in I.

An explanation for these distortions in terms of packing effects also can be ruled out considering the "open" structure of the lattice. More convincing evidence that packing forces are not the origin of these distortions derives from the fact that with a different counterion (Et_4N^+) and in a different lattice,[37] the $Fe(SC_6H_5)_4^{2-}$

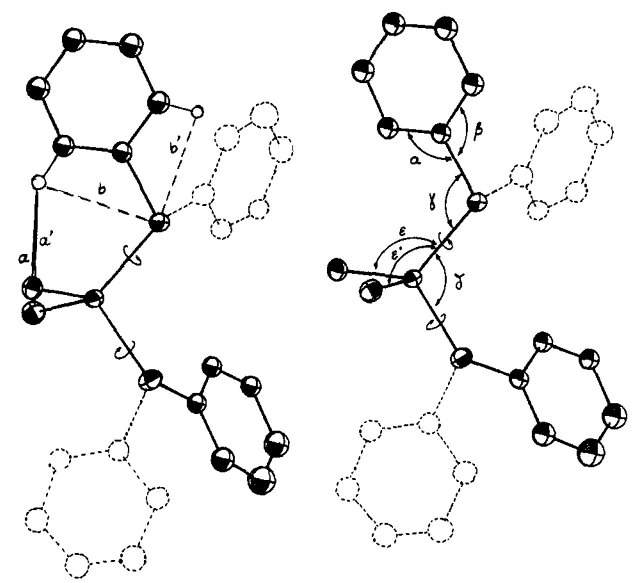

Figure 6. Intramolecular contacts (a) and angles (b) in the $[M(SC_6H_5)_4]^{2-}$ complex anions. The phenyl rings in dotted lines represent sterically equivalent positions possible through rotation about the M–S bond by ca. 120° (three such positions are available for each phenyl ring). Two of the phenyl rings have been omitted for clarity.

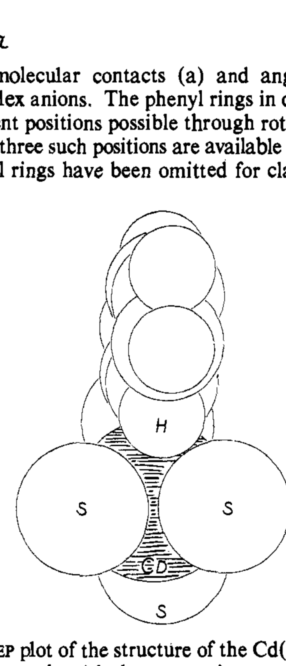

Figure 7. An ORTEP plot of the structure of the $Cd(SC_6H_5)_4^{2-}$ anion with the atoms drawn to scale with the appropriate covalent radii. Three of the phenyl rings have been omitted for clarity.

and $Zn(SC_6H_5)_4^{2-}$ anions show essentially the same angular distortions. The conclusion that must be reached on the basis of all the structural data is that the distortions must be inherent in the structure of the anions.

The phenyl groups attached to sulfur atoms S_1 and S_2 lie in one plane. This plane is orthogonal to another plane defined by the remaining two phenyl groups and sulfur atoms S_3 and S_4

(36) The esd's of typical C–C bonds in the tetraphenylphosphonium cations range from 0.008 to 0.012 Å. The mean value of the 16 equivalent P(C) to ortho C bonds is 1.385 (17) Å. For the 16 equivalent ortho C–meta C bonds a mean value of 1.400 (17) Å is obtained, and for the 16 meta–para C bonds a mean value of 1.350 (18) Å is obtained. The standard deviation from the mean is obtained as indicated in footnote *a* Table VIII.

(37) Structural details for the $[Et_4N]_2[Fe(SC_6H_5)_4]$ complex as well as for the $[Ph_4P]_2[M(SC_6H_5)_4]$ complexes (M = Cd, Zn, Co, Ni, Mn) will be reported in a forthcoming publication.

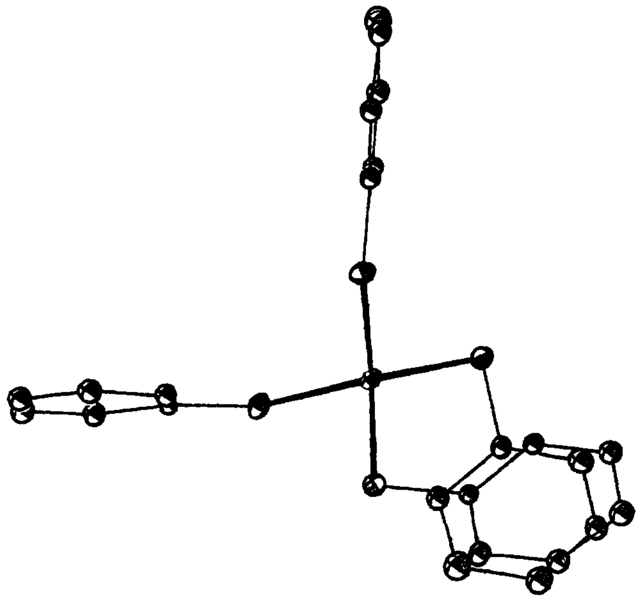

Figure 8. The structure of the $Fe(SC_6H_5)_4^{2-}$ anion in the $[Et_4N]_2Fe(SC_6H_5)_4$ "salt".

(Figure 5). For each phenyl ring, this configuration gives rise to close contacts between the ortho protons, the metal atom, and the sulfur atoms out of the plane of the phenyl rings (Figures 5 and 7, Table VI).

An examination of the data in Table VI shows that each of the proximal orthohydrogen atoms is closer to one of the S atoms (distance *a*) than to the other (distance *a'*) (Figure 6a). Apparently the ortho hydrogen atom chooses one of the two local minima of van der Waals interaction energy and nestles between the metal atom and one of the sulfur atoms (Figure 7).

Typical van der Waals radii are $R_S = 1.84$ Å[34] and $R_M \geq 2$ Å. The distances given in Table VI (Figure 6a) clearly show overlap of the assumed van der Waals radii.

The effects of the ortho hydrogen atom close contacts are aptly demonstrated in the angular distortions found in the $[M(SC_6H_5)_4]^{2-}$ anions (Table VII, Figure 6b). A consideration of *all* phenyl rings and the appropriate ortho hydrogen interactions shows that the two angles ϵ and ϵ' assume values greater than the tetrahedral angle, while δ is always smaller than the tetrahedral angle. In concert with this apparent strain are the values of angles α and β. For unstrained systems α and β are expected to be 120°. For all $M(SC_6H_5)_4^{2-}$ anions allowed to refine with the $S-C_6H_5$ rings fixed as rigid hexagonal groups with an overall group temperature factor, α is greater and β is smaller than 120° (Table VII). For the $Fe(SPh)_4^{2-}$ anion, refinement of the carbom atoms in the $S-C_6H_5$ rings individually with anisotropic temperature factors still shows α greater than β. In this refinement model, both angles are greater than 120° (Table VII), however the four internal C-C-C angles at the carbon atoms attached to the S atoms are significantly smaller than 120° with a mean value of 116.5 (3)°. This deviation of the S-Ph rings from the ideal hexagonal geometry is not evident in the phenyl rings of the phosphonium cations where the corresponding C-C-C angles for the eight independent phenyl rings show a mean value of 119.2 (8)°.

A final systematic distortion apparent in Table VI and VII and indicative of van der Waals repulsions is that for the shortest ortho hydrogen–sulfur distances (*a*) the corresponding S-M-S angles (ϵ) are always larger than the angles (ϵ') corresponding to the longer ortho hydrogen distances (*a'*) (Figure 6).

The same interactions between ortho hydrogen atoms and sulfur and metal atoms are present in the structure of the Et_4N^+ salt of I (Figure 8).[37] With a nearly planar MSC_6H_5 unit there exist three reasonable, equivalent conformations of the phenyl rings in the $M(SC_6H_5)_4^{2-}$ anions. One of these conformations is shown in Figure 5. The second conformation found in the Et_4N^+ salts and shown in Figures 6 and 8 is obtained by simply rotating two

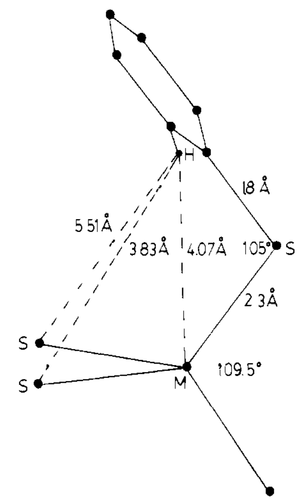

Figure 9. Intramolecular distances in a hypothetical $M(SC_6H_5)_4^{2-}$ structure with a perpendicular ligand orientation.

of the $S_iC_6H_5$– groups about the $M-S_i$ bonds by ca. ±120°.

An alternate anion configuration which eliminates all close intramolecular contacts is one in which the M–S bond is in a plane perpendicular to the phenyl rings plane (Figure 9). All structural data indicate that the parallel mode is the preferred mode of binding. A similar preference is observed with the p-$CH_3C_6H_5S^-$ ligand in the structure of the $[Fe_2S_2(S\text{-}p\text{-tolyl})_4]^{2-}$ complex.[38] In the latter complex the distortions observed in the $Fe^{II}S_4$ coordination sphere are exactly analogous to those reported for I. It should be noted that in the structure of the $[Fe_2S_2(S_2\text{-}o\text{-xyl})_2]^{2-}$ complex, where no intramolecular hydrogen interactions are possible, the deviations of the $Fe^{III}S_4$ units from tetrahedral symmetry are minimal. In comparison to I relatively small distortions from T_d symmetry also are observed in the structures of the $[Fe(S_2\text{-}o\text{-xyl})_2]^-$ and $[Fe(S_2\text{-}o\text{-xyl})_2]^{2-}$ complexes.[19]

A possible reason for the preferred planar binding of the S–Ar ligands is a π type of interaction by the S atom long-pair electrons and the aromatic π system. An ab initio calculation of phenol shows[39] the totally planar configuration, 5 kcal/mol, lower in energy than the configuration with the C–O–H plane perpendicular to the benzene ring. The stability of the planar configuration is attributed to this π type of interaction. The magnitude of an analogous interaction with S atoms would be less than that with oxygen atoms but apparently is enough to cause the ligand to bind in a planar fashion.

It is expected that, as the central atom–S bond becomes shorter, the parallel mode of the $-SC_6H_5$ binding results in considerable strain which eventually, and at the lower limits, forces the phenyl ring out of the plane of the central atom. This is exactly what is found in the structure of the $C(SC_6H_5)_4$ molecule[40] ($\overline{C-S}$ = 1.826 Å) where now the phenyl rings are twisted toward an approximate orthogonal orientation relative to the C–S bonds.

(II) $[Ph_4P]_2[Fe(S_2C_4O_2)_2]$. A distorted FeS_4 central unit is observed in the structure of the $Fe(S_2C_4O_2)_2^{2-}$ as well. The mean Fe–S bond length (2.389 (7) Å) is appreciably longer than corresponding values observed in I and the $[Fe(S_2\text{-}o\text{-xyl})_2^{2-}]$ anion.[19] The angular distortions in the FeS_4 tetrahedron are illustrated in the wide range of the S–Fe–S angles (95.53–124.84°). The smaller of these angles 95.53 and 95.84° are associated with the intra chelate S1–Fe–S2 and S3–Fe–S4 angles, respectively (Figure 2).

Certain structural features of the ligand in II are compared to those found in the structures of the $Cu_8(Dts)_6^{4-}$ and $Ni(Dts)_2^{2-}$ complexes (Table VIII). The cyclobutenone internal ring angles

(38) Mayerle, J. J.; Denmark, S. E.; DePamphilis, B. V.; Ibers, J. A.; Holm, R. H. *J. Am. Chem. Soc.* **1975**, *97*, 1032.
(39) Richards, R.; Walker, S.; Hinkley, T. *J. Am. Chem. Soc.* **1972**, *94*, 1496.
(40) Kato, Von K. *Acta Crystallogr., Sect. B* **1972**, *B28*, 606.

Table II. Positional and Thermal Parameters and Their Standard Deviations in $[Fe(SPh)_4][PPh_4]_2$ [a]

atom	x	y	z	B	atom	x	y	z	B
Fe	0.21508 (6)	0.41196 (5)	0		H(11)	0.3078	0.2739	−0.1692	7.000
S1	0.2821 (1)	0.3247 (1)	−0.06178 (9)		H(12)	0.3812	0.3266	−0.246	7.000
S2	0.2373 (1)	0.3388 (1)	0.07853 (9)		H(13)	0.4405	0.4485	−0.2455	7.000
S3	0.2848 (2)	−0.4672 (1)	0.0083 (1)		H(14)	0.4294	0.5222	−0.1686	7.000
S4	0.0532 (1)	0.4435 (1)	−0.02010 (9)		H(15)	0.356	0.4701	−0.0912	7.000
P1	0.7784 (1)	0.40943 (9)	0.17930 (8)		H(21)	0.1266	0.4726	0.0924	7.000
P2	0.7488 (1)	0.38528 (9)	−0.18901 (9)		H(22)	0.0458	0.5306	0.165	7.000
C1-1	0.3273 (4)	0.3670 (4)	−0.1204 (3)		H(23)	0.0507	0.474	0.2481	7.000
C2-1	0.3322 (5)	0.3249 (4)	−0.1679 (4)		H(24)	0.1342	0.3598	0.261	7.000
C3-1	0.3767 (6)	0.3559 (6)	−0.2134 (3)		H(25)	0.2124	0.3028	0.1887	7.000
C4-1	0.4118 (6)	0.4281 (6)	−0.2135 (4)		H(31)	0.4251	0.4106	0.0023	7.000
C5-1	0.4044 (5)	0.4714 (4)	−0.1674 (4)		H(32)	0.5957	0.4059	0.0013	7.000
C6-1	0.3614 (5)	0.4406 (4)	−0.1222 (3)		H(33)	0.6820	0.5241	0.0080	7.000
C1-2	0.1780 (5)	0.3825 (4)	0.1327 (3)		H(34)	0.6027	0.6368	0.0185	7.000
C2-2	0.1279 (5)	0.4498 (4)	0.1277 (3)		H(35)	0.4398	0.6346	0.0179	7.000
C3-2	0.0803 (5)	0.4838 (4)	0.1707 (3)		H(41)	−0.1484	0.4141	−0.0132	7.000
C4-2	0.0835 (5)	0.4502 (5)	0.2200 (4)		H(42)	−0.2448	0.3058	−0.0179	7.000
C5-2	0.1332 (6)	0.3826 (5)	0.2270 (3)		H(43)	−0.1746	0.1858	−0.031	7.000
C6-2	0.1791 (5)	0.3492 (4)	0.1843 (3)		H(44)	−0.0096	0.1744	−0.0365	7.000
C1-3	0.4149 (7)	0.5253 (6)	0.0106 (3)		H(45)	0.0896	0.2817	−0.0305	7.000
C2-3	0.4621 (8)	0.4565 (8)	0.0068 (4)		H(51)	−0.100	−0.5496	0.0894	5.656
C3-3	0.563 (1)	0.4536 (9)	0.0062 (5)		H(52)	−0.0773	−0.4348	0.0379	5.656
C4-3	0.615 (1)	0.526 (2)	0.0105 (8)		H(53)	−0.1680	−0.3288	0.0593	5.656
C5-3	0.564 (2)	0.589 (1)	0.0155 (7)		H(54)	−0.2802	−0.3308	0.1258	5.656
C6-3	0.470 (1)	0.5874 (7)	0.0152 (4)		H(55)	−0.3073	−0.4433	0.1755	5.656
C1-4	−0.0172 (5)	0.3597 (5)	−0.0207 (2)		H(61)	−0.031	0.3599	0.1483	4.708
C2-4	−0.1200 (6)	0.3647 (6)	−0.0167 (3)		H(62)	0.031	0.2517	0.1058	4.708
C3-4	−0.1759 (6)	0.2992 (9)	−0.0199 (3)		H(63)	−0.0715	0.1528	0.0818	4.708
C4-4	−0.1336 (9)	0.2291 (6)	−0.0274 (3)		H(64)	−0.2348	0.1613	0.0967	4.708
C5-4	−0.0361 (7)	0.2237 (5)	−0.0305 (3)		H(65)	−0.3004	0.270	0.1374	4.708
C6-4	0.0210 (5)	0.2870 (5)	−0.0275 (3)		H(71)	−0.3431	0.3705	0.2672	6.096
C1-5	−0.2037 (4)	−0.5082 (4)	0.1376 (3)	4.3 (1)	H(72)	−0.5097	0.3444	0.2753	6.096
C2-5	−0.1361 (5)	−0.5049 (4)	0.0978 (3)	5.0 (1)	H(73)	−0.6088	0.3528	0.2015	6.096
C3-5	−0.1231 (5)	−0.4375 (4)	0.0668 (3)	5.4 (2)	H(74)	−0.5522	0.3882	0.1207	6.096
C4-5	−0.1768 (5)	−0.3748 (4)	0.0800 (3)	6.0 (2)	H(75)	−0.386	0.4167	0.1087	6.096
C5-5	−0.2435 (6)	−0.3757 (5)	0.1193 (3)	6.1 (2)	H(81)	−0.2120	0.5325	−0.7466	5.167
C6-5	−0.2594 (5)	−0.4422 (5)	0.1488 (3)	6.4 (2)	H(82)	−0.1535	0.5465	−0.6594	5.167
C1-6	−0.1733 (5)	0.3252 (3)	0.1479 (3)	4.0 (1)	H(83)	−0.0705	0.4473	−0.6186	5.167
C2-6	−0.0731 (5)	0.3193 (4)	0.1386 (3)	4.6 (1)	H(84)	−0.0449	0.335	−0.6622	5.167
C3-6	−0.0363 (5)	0.2558 (4)	0.1137 (3)	4.9 (1)	H(85)	−0.1078	0.3179	−0.7508	5.167
C4-6	−0.0971 (5)	0.1971 (4)	0.0997 (3)	4.9 (1)	H(91)	−0.393	0.2932	−0.2409	4.874
C5-6	−0.1932 (5)	0.2017 (4)	0.1081 (3)	4.9 (1)	H(92)	−0.4795	0.2995	−0.3218	4.874
C6-6	−0.2326 (5)	0.2664 (4)	0.1321 (3)	4.5 (1)	H(93)	−0.4519	0.4008	−0.3804	4.874
C1-7	−0.3482 (5)	0.3958 (4)	0.1886 (3)	4.3 (1)	H(94)	−0.3427	0.4958	−0.3595	4.874
C2-7	−0.3854 (5)	0.3745 (4)	0.2376 (3)	5.0 (1)	H(95)	−0.2580	0.491	−0.2789	4.874
C3-7	−0.4841 (6)	0.3586 (4)	0.2422 (3)	6.7 (2)	H(01)	−0.0944	0.3380	−0.1239	4.665
C4-7	−0.5421 (6)	0.3645 (5)	0.1989 (4)	7.3 (2)	H(02)	0.0688	0.3078	−0.139	4.665
C5-7	−0.5090 (6)	0.3851 (5)	0.1513 (3)	7.2 (2)	H(03)	0.1293	0.307	−0.2257	4.665
C7-7	−0.4108 (6)	0.4020 (4)	0.1441 (3)	6.3 (2)	H(04)	0.0286	0.331	−0.2980	4.665
C1-8	−0.1661 (4)	0.4232 (3)	−0.7559 (3)	4.2 (1)	H(05)	−0.1339	0.3624	−0.2842	4.665
C2-8	−0.1791 (5)	0.4919 (4)	−0.7289 (3)	5.4 (2)	H(11)	−0.1152	−0.5306	−0.1277	6.238
C3-8	−0.1437 (5)	0.5000 (4)	−0.6769 (3)	5.3 (1)	H(12)	−0.1177	−0.4102	−0.0838	6.238
C4-8	−0.0955 (5)	0.4410 (4)	−0.6530 (3)	5.5 (2)	H(13)	−0.2555	−0.3356	−0.0896	6.238
C5-8	−0.0795 (5)	0.3752 (4)	−0.6784 (3)	5.4 (2)	H(14)	−0.3838	−0.3731	−0.1367	6.238
C6-8	−0.1169 (5)	0.3645 (4)	−0.7312 (3)	5.2 (1)	H(15)	−0.383	−0.493	−0.1826	6.238
C1-9	−0.3179 (4)	0.3907 (3)	−0.2507 (2)	3.7 (1)	H(21)	−0.418	0.3887	−0.1225	6.265
C2-9	−0.3827 (5)	0.3345 (4)	−0.2641 (3)	4.8 (1)	H(22)	−0.5065	0.2911	−0.0751	6.265
C3-9	−0.4343 (5)	0.3389 (4)	−0.3125 (3)	4.9 (1)	H(23)	−0.4525	0.1684	−0.0773	6.265
C4-9	−0.4172 (5)	0.3984 (4)	−0.3462 (3)	5.6 (2)	H(24)	−0.3126	0.1358	−0.1185	6.265
C5-9	−0.3526 (5)	0.4551 (4)	−0.3344 (3)	5.2 (1)	H(25)	−0.2223	0.2304	−0.1651	6.265
C6-9	−0.3026 (4)	0.4514 (4)	−0.2867 (3)	4.5 (1)					
C1-10	−0.1292 (4)	0.3538 (3)	−0.2014 (3)	3.9 (1)					
C2-10	−0.0696 (5)	0.3370 (3)	−0.1585 (2)	4.2 (1)					
C3-10	0.0272 (5)	0.3194 (4)	−0.1672 (3)	5.2 (2)					
C4-10	0.0633 (5)	0.3186 (4)	−0.2187 (3)	4.9 (1)					
C5-10	0.0038 (5)	0.3328 (4)	−0.2616 (3)	4.9 (1)					
C6-10	−0.0931 (4)	0.3512 (4)	−0.2539 (3)	4.3 (1)					
C1-11	−0.2502 (5)	−0.5231 (3)	−0.1580 (3)	4.4 (1)					
C2-11	−0.1711 (5)	−0.4984 (4)	−0.1289 (3)	5.5 (2)					
C3-11	−0.1726 (6)	−0.4275 (5)	−0.1033 (4)	7.4 (2)					
C4-11	−0.2534 (6)	−0.3837 (5)	−0.1061 (4)	7.1 (2)					
C5-11	−0.3282 (6)	−0.4059 (5)	−0.1347 (4)	7.2 (2)					
C6-11	−0.3288 (6)	−0.4763 (4)	−0.1611 (3)	6.3 (2)					
C1-12	−0.3110 (5)	0.3175 (3)	−0.1473 (3)	4.3 (1)					
C2-12	−0.3947 (6)	0.3376 (4)	−0.1202 (3)	6.6 (2)					
C3-12	−0.4486 (6)	0.2788 (5)	−0.0928 (4)	7.7 (2)					
C4-12	−0.4162 (6)	0.2074 (5)	−0.0939 (4)	7.0 (2)					
C5-12	−0.3336 (6)	0.1870 (5)	−0.1184 (3)	6.6 (2)					
C6-12	−0.2806 (4)	0.2433 (4)	−0.1462 (3)	4.8 (1)					

Table II (*Continued*)

atom	$B(11)$	$B(22)$	$B(33)$	$B(12)$	$B(13)$	$B(23)$
Fe	4.68 (5)	5.10 (5)	4.64 (5)	−0.07 (4)	0.54 (4)	−0.25 (4)
S1	6.6 (1)	5.2 (1)	7.1 (1)	−0.16 (8)	2.46 (9)	−0.43 (9)
S2	5.4 (1)	5.24 (9)	5.7 (1)	0.30 (8)	0.39 (8)	0.40 (8)
S3	9.5 (1)	5.5 (1)	6.5 (1)	−1.30 (9)	1.4 (1)	−0.5 (1)
S4	5.7 (1)	7.2 (1)	5.5 (1)	0.85 (8)	−0.45 (8)	−0.12 (8)
P1	4.14 (9)	4.16 (8)	4.3 (1)	−0.02 (7)	0.24 (7)	−0.02 (7)
P2	3.96 (8)	4.32 (8)	3.88 (8)	0.13 (7)	0.00 (6)	−0.04 (7)
C1-1	3.6 (3)	5.3 (4)	4.7 (4)	0.6 (3)	0.9 (3)	−1.3 (3)
C2-1	4.2 (4)	6.7 (4)	8.0 (6)	0.4 (3)	0.6 (4)	−1.3 (4)
C3-1	6.8 (5)	8.8 (6)	4.7 (4)	1.1 (4)	0.6 (4)	−1.5 (4)
C4-1	6.1 (5)	7.1 (5)	6.2 (5)	2.2 (4)	0.3 (4)	1.9 (4)
C5-1	5.3 (4)	6.4 (4)	6.3 (5)	0.5 (3)	0.6 (4)	0.4 (4)
C6-1	4.8 (4)	5.7 (4)	5.1 (4)	0.4 (3)	0.2 (3)	−0.9 (3)
C1-2	4.2 (3)	3.7 (3)	4.9 (4)	−1.3 (3)	0.0 (3)	0.6 (3)
C2-2	4.5 (4)	5.4 (4)	4.6 (4)	−1.0 (3)	0.1 (3)	−0.5 (3)
C3-2	5.1 (4)	5.5 (4)	5.3 (4)	−0.8 (3)	−0.9 (3)	0.4 (4)
C4-2	4.1 (4)	5.6 (4)	7.7 (6)	−1.2 (3)	0.4 (3)	−1.9 (4)
C5-2	5.6 (4)	6.9 (5)	5.1 (5)	−2.5 (4)	0.7 (3)	0.9 (4)
C6-2	4.2 (4)	5.6 (4)	6.1 (5)	−1.2 (3)	0.5 (3)	0.3 (4)
C1-3	8.0 (6)	9.2 (6)	3.8 (4)	−3.4 (5)	0.6 (3)	−0.2 (4)
C2-3	6.9 (6)	13.8 (9)	6.9 (6)	−1.3 (6)	−1.1 (5)	0.2 (6)
C3-3	8.3 (8)	19.1 (12)	7.3 (6)	0.9 (7)	−2.0 (6)	2.1 (7)
C4-3	9.3 (13)	34.4 (32)	7.4 (9)	−9.1 (15)	−2.2 (8)	4.4 (16)
C5-3	11.6 (15)	20.9 (17)	6.5 (8)	−8.0 (12)	−1.9 (9)	3.6 (9)
C6-3	12.1 (9)	15.3 (9)	5.9 (6)	−7.8 (8)	−0.3 (5)	2.6 (5)
C1-4	3.9 (4)	9.0 (5)	2.8 (3)	−0.5 (3)	−0.2 (2)	−0.9 (3)
C2-4	5.5 (5)	10.3 (6)	3.3 (4)	0.3 (4)	0.0 (3)	−0.4 (3)
C3-4	3.6 (4)	15.2 (10)	4.6 (4)	−1.4 (6)	−0.7 (3)	0.6 (5)
C4-4	8.5 (7)	9.9 (7)	3.7 (4)	−1.5 (5)	0.0 (4)	0.8 (4)
C5-4	6.1 (5)	9.2 (6)	3.8 (4)	−0.3 (4)	−0.9 (3)	0.5 (4)
C6-4	5.0 (4)	6.6 (4)	4.6 (4)	−0.8 (4)	−0.0 (3)	0.4 (3)

[a] Calculated standard deviations are indicated in parentheses. The thermal parameters are in units of square angstroms. The temperature factor has the form $T = -\Sigma(^1/_4 B(IJ)H(I)H(J)\mathrm{ASTAR}(I)\mathrm{ASTAR}(J))$ for the anisotropic case. $T = -B((\sin\theta)/\lambda)^2$ for the isotropic case. H is the Miller Index, ASTAR is the reciprocal cell length, and I and J are cycled 1 through 3.

do not differ appreciably in the three structures; however, the magnitudes of the S–C–C endo-chelate and exo-chelate angles show pronounced variations. These variations also are reflected in a wide range in the "bite" size of the $S_2C_4O_2^{2-}$ ligand. It appears likely, that the observed variations in the S–C–C angles and, consequently, of the ligand bite size are determined primarily by the coordination geometry around the chelated metal atom, the directional character of the sulfur donor electron pairs (C–S–M angle), and the M–S bond length.

In the present structure the ligand is slightly distorted from the "ideal" geometry with a C–C–S endo angle of 137.6° compared to an expected value of ~134° in the free ligand. At a Fe–S distance of ~2.39 Å the observed S–Fe–S angle is 95.5° and the C–S–Fe angle is ~92°. Any further "opening up" of the S–Fe–S angle *at a fixed Fe–S bond length* would give rise to smaller C–S–Fe angles. Thus if the ligand was to "open up" so that it resembles in geometry the ligands in the $(Cu_8(Dts)_6)^{4-}$ cluster (C–C–S = 129.9° and a bite of 3.92 Å), the S–Fe–S angle would be ~112°; however, the C–S–Fe angle would have to have the very acute value of 75°.

As observed in the structures of numerous 1,2-dithiolene complexes[41] the "ethylenic" C=C length in the $S_2C_4O_2^{2-}$ coordinated ligand is slightly longer than a pure double bond and the C–S bond lengths are slightly shorter than a single bond. For the 1,2-dithiolene complexes the M–S–C angles range from 101.5 to 110°. Under the assumption that the hybridized orbitals used by the sulfur donors in the 1,2-dithiolenes are similar to those present in sulfur donors of the $S_2C_4O_2^{2-}$ ligand, the Fe–S–C angle of 92° found in the present structure may be close to a lower limit for the size of this angle.

On the basis of the above considerations, it is apparent that the inequivalence of the S–Fe–S angles in the FeS_4 core arises from the strain limitations of the $S_2C_4O_4^{2-}$ ligands. The structure of the $S_2C_4O_2^{2-}$ ligand has been described in detail elsewhere[20] and will not be discussed any further. The same applies for the structures of the two Ph_4P^+ cations which are unexceptional and will not be discussed.

Mössbauer and Magnetic Susceptibility Results. Preliminary results on zero magnetic field spectra have been reported elsewhere.[24] These measurements showed that complex I displays the same isomer shift and quadrupole splitting with those of reduced rubredoxin.[42] Spectra of the two complexes at high magnetic fields are shown in Figure 10. A spectrum of the Rd_{red} taken by Schultz and Debrunner[43] at the same temperature and magnetic field is also included for comparison. The similarity of the spectrum of I to that of the protein is striking. The difference in the absorption near the velocity of 2 mm/s arises from the different geometry of the external magnetic field which was used for the two cases.

The spin Hamiltonian appropriate to the lowest orbital singlet spin quintet electronic level of the energy diagram depicted in Figure 11 is

$$H_{el} = D[S_z^2 - \tfrac{1}{3}[S(S+1)]] + E(S_x^2 - S_y^2) + \beta\vec{S}\cdot\tilde{g}\mathbf{H}_{ap} \quad (1)$$

where D and E represent the familiar axial and rhombic crystal field parameters. The line shapes of the magnetically perturbed spectra (Figure 10) have been calculated from the nuclear spin Hamiltonian

$$H_N = \langle\vec{S}\rangle\cdot\mathbf{A}\cdot\vec{\mathbf{I}} + \frac{e^2qQ}{12}\left[3I_z^2 - \frac{15}{4} + \eta(I_x^2 - I_y^2)\right] - g_n\beta_n\vec{H}_{ap}\cdot\vec{\mathbf{I}} + \delta \quad (2)$$

where the expectation value of the electronic spin $\langle\vec{S}\rangle$ can be calculated by diagonalization of the Hamiltonian (1). **A** is the

(41) Eisenberg, R. *Prog. Inorg. Chem.* **1970**, *12*, 295.

(42) Rao, K. K.; Evans, M. C. W.; Cammack, R.; Hall, D. O.; Thomson, C. L.; Jackson, P. J.; Johnson, C. E. *Biochem. J.* **1972**, *129*, 1063.

(43) Schultz, C.; Debrunner, P. G. *J. Phys. (Orsay, France)* **1976**, *37*, C6-153.

Table III. Positional and Thermal Parameters and Their Standard Deviations in $[Ph_4P]_2[Fe(S_2C_4O_2)_2]$[a]

atom	*x*	*y*	*z*	*B*(11)	*B*(22)	*B*(33)	*B*(12)	*B*(13)	*B*(23)
Fe	0.26560 (8)	0.09730 (8)	0.05359 (7)	5.01 (8)	4.26 (7)	4.46 (6)	−0.05 (6)	2.11 (6)	−0.01 (5)
S1	0.2772 (2)	0.0130 (1)	−0.0472 (1)	7.2 (2)	4.8 (1)	5.1 (1)	0.3 (1)	3.4 (1)	0.0 (1)
S2	0.2838 (2)	−0.0076 (1)	0.1478 (1)	5.9 (2)	4.6 (1)	4.0 (1)	−0.8 (1)	1.7 (1)	0.08 (9)
S3	0.3511 (2)	0.2111 (1)	0.1067 (1)	4.6 (1)	4.8 (1)	6.6 (1)	−0.2 (2)	2.2 (1)	−0.58 (1)
S4	0.1385 (2)	0.1674 (1)	0.0218 (1)	4.7 (1)	5.2 (1)	5.6 (1)	−0.1 (1)	1.7 (1)	−0.38 (1)
P1	0.5521 (1)	0.0644 (1)	0.3563 (1)	3.9 (1)	4.4 (1)	3.7 (1)	−0.16 (9)	1.4 (1)	0.16 (9)
P2	−0.0154 (1)	0.1963 (1)	0.2239 (1)	4.2 (1)	3.6 (1)	3.9 (1)	0.3 (1)	1.5 (1)	−0.05 (9)
O1	0.0973 (5)	0.3521 (4)	0.1031 (5)	7.1 (5)	6.2 (4)	13.4 (6)	0.8 (4)	5.5 (5)	−1.0 (4)
O2	0.2962 (5)	0.3915 (4)	0.1876 (4)	8.6 (5)	4.8 (4)	6.9 (4)	−0.8 (4)	2.8 (4)	−1.5 (3)
O3	0.2799 (5)	−0.2054 (4)	−0.0572 (4)	10.6 (6)	5.1 (4)	8.7 (5)	−1.0 (4)	6.0 (4)	−2.0 (3)
O4	0.2927 (5)	−0.2214 (4)	0.1262 (4)	9.3 (5)	4.2 (4)	7.3 (4)	0.2 (3)	2.6 (4)	1.3 (3)
C1	0.2702 (6)	0.2648 (5)	0.1086 (5)	4.3 (6)	3.9 (5)	4.2 (4)	−0.7 (4)	1.6 (4)	0.3 (4)
C2	0.1860 (6)	0.2480 (5)	0.0747 (5)	4.7 (6)	3.7 (5)	4.7 (5)	1.0 (4)	2.4 (4)	1.5 (4)
C3	0.1612 (7)	0.3215 (6)	0.1057 (6)	5.3 (7)	3.7 (5)	7.2 (6)	−0.4 (5)	3.3 (6)	0.5 (4)
C4	0.2543 (7)	0.3411 (6)	0.1450 (6)	7.0 (8)	4.1 (5)	4.9 (5)	0.4 (5)	3.2 (5)	0.1 (4)
C5	0.2856 (5)	−0.0710 (5)	0.0080 (6)	4.3 (5)	4.3 (6)	5.9 (6)	−0.2 (4)	2.9 (4)	−0.6 (4)
C6	0.2885 (5)	−0.0792 (5)	0.0847 (5)	4.0 (5)	4.2 (6)	4.8 (5)	−0.7 (4)	2.0 (4)	−0.1 (4)
C7	0.2912 (6)	−0.1680 (6)	0.0815 (6)	4.2 (6)	4.3 (6)	6.3 (6)	−0.2 (4)	2.0 (5)	−0.0 (5)
C8	0.2850 (6)	−0.1594 (6)	−0.0045 (6)	5.6 (6)	4.8 (6)	6.5 (6)	−0.6 (5)	3.1 (5)	−0.7 (5)

atom	*x*	*y*	*z*	*B*	atom	*x*	*y*	*z*	*B*
C9	0.5655 (5)	0.0725 (5)	0.2643 (4)	3.6 (2)	H(11)	0.6737	0.1323	0.3025	5.168
C10	0.6321 (6)	0.1126 (5)	0.2568 (5)	5.0 (2)	H(12)	0.6854	0.149	0.1785	5.168
C11	0.6391 (6)	0.1225 (6)	0.1835 (5)	5.4 (2)	H(13)	0.5851	0.1015	0.0694	5.168
C12	0.5798 (6)	0.0944 (6)	0.1192 (5)	5.5 (2)	H(14)	0.4710	0.0378	0.0764	5.168
C13	0.5124 (7)	0.0567 (6)	0.1230 (6)	6.0 (2)	H(15)	0.4566	0.0192	0.2011	5.168
C14	0.5035 (6)	0.0455 (6)	0.1969 (5)	5.4 (2)	H(21)	0.6919	0.1553	0.4432	5.376
C15	0.6478 (5)	0.0415 (5)	0.4323 (5)	4.0 (2)	H(22)	0.8244	0.1229	0.5357	5.376
C16	0.7056 (6)	0.1019 (6)	0.4611 (5)	5.2 (2)	H(23)	0.8542	−0.0045	0.5752	5.376
C17	0.7838 (7)	0.0825 (6)	0.5158 (6)	6.2 (2)	H(24)	0.761	−0.1054	0.5335	5.376
C18	0.8009 (7)	0.0074 (6)	0.5388 (6)	6.3 (2)	H(25)	0.6288	−0.0772	0.4412	5.376
C19	0.7465 (6)	−0.0523 (6)	0.5145 (5)	5.8 (2)	H(31)	0.5394	−0.0982	0.310	4.662
C20	0.6684 (6)	−0.0357 (5)	0.4599 (5)	4.7 (2)	H(32)	0.4471	−0.2021	0.3033	4.662
C21	0.4802 (5)	−0.0132 (5)	0.3507 (4)	3.6 (2)	H(33)	0.334	−0.1799	0.3396	4.662
C22	0.4928 (6)	−0.0890 (6)	0.3248 (5)	4.9 (2)	H(34)	0.3108	−0.0543	0.3818	4.662
C23	0.4380 (6)	−0.1504 (6)	0.3208 (5)	5.8 (2)	H(35)	0.4004	0.0506	0.3872	4.662
C24	0.3713 (6)	−0.1374 (6)	0.3421 (5)	5.2 (2)	H(41)	0.5384	0.1329	0.4946	5.138
C25	0.3575 (6)	−0.0630 (5)	0.3670 (5)	4.6 (2)	H(42)	0.4908	0.2562	0.5248	5.138
C26	0.4106 (5)	−0.0011 (5)	0.3704 (4)	4.0 (2)	H(43)	0.4433	0.3536	0.4308	5.138
C27	0.5153 (5)	0.1588 (5)	0.3790 (4)	3.5 (2)	H(44)	0.4379	0.3308	0.3050	5.138
C28	0.5179 (6)	0.1730 (5)	0.4554 (5)	5.1 (2)	H(45)	0.4840	0.2081	0.2707	5.138
C29	0.4897 (6)	0.2461 (6)	0.4731 (5)	5.7 (2)	H(51)	0.1021	0.2779	0.3529	4.992
C30	0.4617 (6)	0.3037 (6)	0.4178 (6)	5.8 (2)	H(52)	0.2443	0.2795	0.4075	4.992
C31	0.4586 (6)	0.2899 (6)	0.3435 (6)	6.0 (2)	H(53)	0.3228	0.2058	0.3523	4.992
C32	0.4856 (5)	0.2177 (5)	0.3226 (5)	4.8 (2)	H(54)	0.2588	0.1311	0.2394	4.992
C33	0.0941 (5)	0.2026 (5)	0.2634 (4)	3.5 (2)	H(55)	0.1151	0.1288	0.1833	4.992
C34	0.1338 (6)	0.2477 (6)	0.3295 (5)	5.4 (2)	H(61)	−0.151	0.088	0.1921	5.522
C35	0.2179 (7)	0.2485 (6)	0.3617 (6)	6.2 (2)	H(62)	−0.2045	0.0089	0.2711	5.522
C36	0.2645 (6)	0.2051 (6)	0.3293 (5)	5.8 (2)	H(63)	−0.1365	0.0077	0.4031	5.522
C37	0.2265 (6)	0.1608 (6)	0.2624 (5)	5.2 (2)	H(64)	−0.0177	0.0785	0.4630	5.522
C38	0.1415 (5)	0.1596 (5)	0.2293 (4)	3.9 (2)	H(65)	0.0363	0.1569	0.3836	5.522
C39	−0.0523 (5)	0.1300 (5)	0.2807 (4)	3.7 (2)	H(71)	−0.150	0.2522	0.2621	4.922
C40	−0.1236 (6)	0.0863 (6)	0.2474 (5)	5.3 (2)	H(72)	−0.2051	0.3797	0.2731	4.922
C41	−0.1554 (6)	0.0392 (6)	0.2936 (6)	6.4 (2)	H(73)	−0.1460	0.4898	0.2460	4.922
C42	−0.1148 (7)	0.0393 (6)	0.3714 (6)	6.7 (2)	H(74)	−0.0317	0.4847	0.2099	4.922
C43	−0.0446 (6)	0.0807 (6)	0.4076 (6)	6.2 (2)	H(75)	0.0279	0.3576	0.2011	4.922
C44	−0.0128 (6)	0.1271 (5)	0.3604 (5)	4.9 (2)	H(81)	−0.061	0.2734	0.0765	5.062
C45	−0.0575 (5)	0.2940 (5)	0.2312 (4)	3.8 (2)	H(82)	−0.0957	0.2298	−0.0546	5.062
C46	−0.1254 (6)	0.2996 (5)	0.2517 (5)	4.7 (2)	H(83)	−0.0992	0.0952	−0.0805	5.062
C47	−0.1582 (6)	0.3748 (6)	0.2582 (5)	5.4 (2)	H(84)	−0.0721	0.0014	0.0171	5.062
C48	−0.1226 (6)	0.4391 (6)	0.2421 (5)	5.5 (2)	H(85)	−0.0357	0.0435	0.1500	5.062
C49	−0.0555 (7)	0.4368 (6)	0.2209 (6)	5.8 (2)					
C50	−0.0195 (5)	0.3616 (5)	0.2154 (5)	4.4 (2)					
C51	−0.0469 (5)	0.1625 (5)	0.1251 (5)	4.0 (2)					
C52	−0.0631 (6)	0.2176 (5)	0.0648 (5)	4.8 (2)					
C53	−0.0837 (6)	0.1920 (6)	−0.0129 (5)	5.7 (2)					
C54	−0.0857 (6)	0.1125 (6)	−0.0277 (5)	5.5 (2)					
C55	−0.0696 (6)	0.0569 (6)	0.0297 (5)	5.5 (2)					
C56	−0.0481 (6)	0.0815 (5)	0.1085 (5)	4.8 (2)					

[a] See footnote *a* in Table II.

hyperfine constant tensor, η is the asymmetry parameter of the EFG tensor, and δ is the isomer shift.[44]

The parameters of the Hamiltonian (1) and (2) for the complexes I and II have been determined by consistent fittings of the

(44) Details of the analysis of the Mössbauer spectra and the magnetization measurements will be published elsewhere.

(45) Abragam, A.; Bleaney, B. "Electron Paramagnetic Resonance of Transition Ions"; Oxford University Press: London, 1970; p 399.

Table IV. Intramolecular Bond Distances[a] and Angles (Deg) in $[(C_6H_5)_4P]_2Fe(SC_6H_5)_4$ (I)

Bond Distances			
Fe-S1	2.359 (2)	P1-C1-8	1.804 (7)
Fe-S2	2.360 (2)	P2-C1-9	1.794 (6)
Fe-S3	2.338 (2)	P2-C1-10	1.798 (6)
Fe-S4	2.355 (2)	P2-C1-11	1.782 (6)
S1-C1-1	1.752 (7)	P2-C1-12	1.781 (7)
S2-C1-2	1.754 (7)	S1-S2	3.559 (3)
S3-C1-3	1.800 (10)	S1-S3	4.047 (4)
S4-C1-4	1.762 (8)	S1-S4	3.923 (3)
P1-C1-5	1.797 (6)	S2-S3	3.882 (4)
P1-C1-6	1.800 (6)	S2-S4	3.983 (4)
P1-C1-7	1.778 (7)	S3-S4	3.630 (3)
Bond Angles			
S1-Fe-S2	97.89 (9)	C1-5-P1-C1-7	108.6 (4)
S1-Fe-S3	119.00 (10)	C1-5-P1-C1-8	110.6 (4)
S1-Fe-S4	112.67 (10)	C1-6-P1-C1-7	108.0 (4)
S2-Fe-S3	111.47 (11)	C1-6-P1-C1-8	110.0 (4)
S2-Fe-S4	115.27 (9)	C1-7-P1-C1-8	108.6 (4)
S3-Fe-S4	101.34 (10)	C1-9-P2-C1-10	110.4 (4)
Fe-S1-C1-1	114.1 (2)	C1-9-P2-C1-11	109.1 (4)
Fe-S2-C1-2	109.9 (2)	C1-9-P2-C1-12	107.3 (4)
Fe-S3-C1-3	110.3 (4)	C1-10-P2-C1-11	110.1 (4)
Fe-S4-C1-4	109.2 (3)	C1-10-P2-C1-12	109.2 (4)
C1-5-P1-C1-6	111.0 (4)	C1-11-P2-C1-12	110.7 (4)

[a] The numbers following the hyphens in the carbon atom designations indicate the corresponding phenyl rings.

Table V. Intramolecular Bond Distances (Å) and Angles (Deg) in $[(C_6H_5)_4P]_2Fe(S_2C_4O_2)_2$ (II)

Bond Distances			
Fe-S1	2.379 (3)	S1-S2	3.535 (3)
Fe-S2	2.394 (3)	S3-S4	3.550 (4)
Fe-S3	2.396 (3)	S1-S4	4.022 (4)
Fe-S4	2.387 (3)	S1-S3	4.233 (3)
S1-C5	1.701 (9)	S2-S3	3.982 (4)
S2-C6	1.681 (9)	S2-S4	4.015 (4)
S3-C1	1.679 (9)	S1-O3	3.648 (7)
S4-C2	1.692 (10)	S2-O4	3.597 (7)
O1-C3	1.209 (11)	S3-O2	3.624 (7)
O2-C4	1.202 (11)	S4-O1	3.598 (8)
O3-C8	1.208 (10)	O1-O2	3.324 (11)
O4-C7	1.201 (10)	O3-O4	3.283 (10)
C1-C2	1.405 (11)	P1-C9	1.780 (8)
C5-C6	1.389 (11)	P1-C15	1.794 (8)
C1-C4	1.505 (12)	P1-C21	1.778 (8)
C2-C3	1.477 (13)	P1-C27	1.801 (8)
C5-C8	1.492 (13)	P2-C33	1.788 (8)
C6-C7	1.483 (13)	P2-C39	1.784 (8)
C3-C4	1.559 (15)	P2-C45	1.811 (8)
C7-C8	1.541 (14)	P2-C51	1.781 (8)
Bond Angles			
S1-Fe-S2	95.57 (11)	C6-C5-C8	93.0 (8)
S1-Fe-S3	124.86 (13)	C1-C4-C3	86.7 (8)
S1-Fe-S4	115.11 (13)	C4-C3-C2	87.4 (7)
S2-Fe-S3	112.42 (12)	C6-C7-C8	87.4 (7)
S2-Fe-S4	114.23 (12)	C5-C8-C7	86.7 (8)
S3-Fe-S4	95.83 (12)	S3-C1-C4	138.2 (6)
Fe-S1-C5	92.4 (3)	S1-C5-C8	136.8 (5)
Fe-S2-C6	93.1 (3)	S2-C6-C7	138.2 (5)
Fe-S3-C1	91.4 (3)	S4-C2-C3	136.7 (6)
Fe-S4-C2	91.4 (3)	O1-C3-C4	136.3 (9)
S3-C1-C2	129.6 (5)	O2-C4-C3	137.8 (8)
S4-C2-C1	129.5 (5)	O3-C8-C7	135.3 (8)
S1-C5-C6	130.0 (5)	O4-C7-C8	137.4 (8)
S2-C6-C5	128.8 (5)	O1-C3-C2	136.3 (9)
C2-C1-C4	92.2 (8)	O2-C4-C1	135.5 (9)
C3-C2-C1	93.7 (8)	O3-C8-C5	138.0 (8)
C7-C6-C5	92.8 (8)	O4-C7-C6	135.0 (8)

spectra at different temperatures and applied fields and are listed in Table IX. The zero field parameters D and E for I have been measured independently by far-infrared magnetic resonance spectroscopy.[46] The reported values have been kept constant

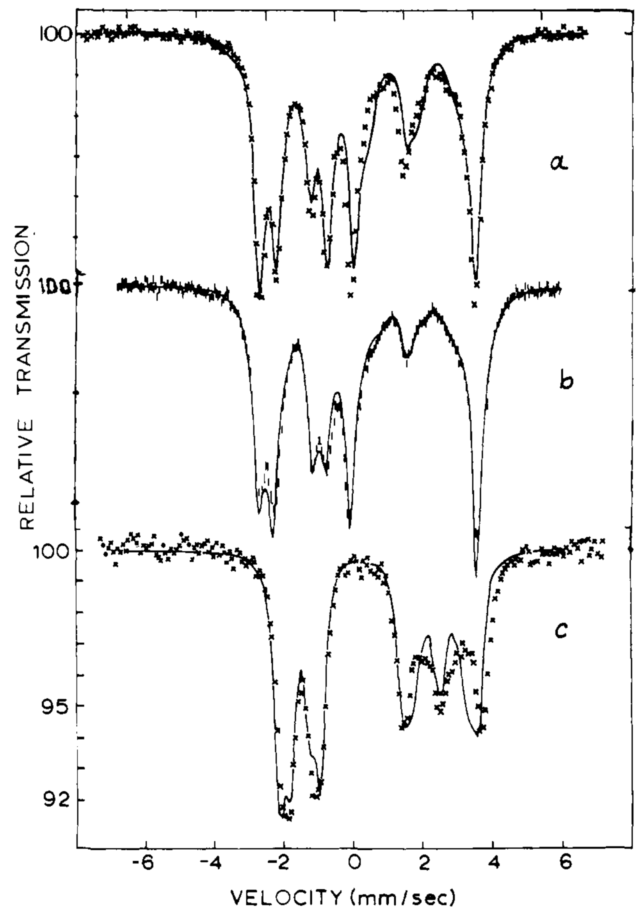

Figure 10. Mössbauer spectra at 4.2 K of (a) $[Fe(SC_6H_5)_4]^{2-}$ in a transverse field of 26 kG, (b) reduced Rd in a parallel field of 24 kG, and (c) $[Fe(S_2C_4O_2)_2]^{2-}$ in a transverse field of 26 kG. The solid lines are simulated spectra calculated with the parameters given in Table I. Spectrum b is reconstructed from ref 41.

during the fitting procedure. In the case of II, however, D and E have been treated as free parameters. In the same table we include also the parameters for reduced rubredoxin extracted from Mössbauer spectra by a similar procedure.[43] The results indicate (Table IX) that the parameter sets for I, II and Rd_{red} are very similar. Of particular interest is the observation that, while there exists a very close agreement in the components A_y and A_z of the magnetic hyperfine tensor and ΔE_Q for I and $(Rd)_{red}$, significantly different values are found for II. As shown in a complete analysis of the electronic structure of the ground-state spin quintet,[45] the magnetically perturbed spectra depend mainly on the value of the A_y, due to the significant rhombic anisotropy ($E/D \simeq 0.25$). The practically identical values found for this parameter in I and Rd_{red} correspond to the striking similarity of their Mössbauer spectra (a and b in Figure 10) and imply very similar electronic structures.

The quadrupole interaction of complex I does not show any substantial temperature variation between 4.2 and 30 K[24] and is in agreement with the results of Rd_{red}. This lack of temperature variation sets a lower limit of the energy separation of the two lowest orbital states at ~ 1000 cm^{-1} which is close to the value of 850 cm^{-1} estimated for the protein by Eaton and Lovenberg[4] from the slight variation of the quadrupole splitting with temperature. Complex II on the other hand shows a substantial temperature variation of the quadrupole splitting which corresponds to an energy separation of the two lowest orbital states of ~ 400 cm^{-1}.

In the framework of the second-order perturbation approximation the zero field splitting parameters can be expressed in terms of the energies of the orbital states (Figure 11) and the spin–orbit coupling constant. A calculation with the values determined from

(46) Champion, P. M.; Sievers, A. J. J. Chem. Phys. 1977, 66, 1819.

Table VI. Hydrogen Atom Interactions in the Tetraphenylphosphonium "Salts" of the Phenyl Mercaptide ($M(SC_6H_5)_4^{2-}$) Complexes

	metal						
dist, Å	Mn	Fe	Co	Ni	Zn	Cd	Fe′[a]
M-S(av)	2.442 (13)	2.353 (9)	2.328 (11)	2.288 (13)	2.353 (14)	2.535 (11)	2.33 (1)
M-H(av)	2.95 (10)	2.98 (8)	2.86 (10)	2.88 (10)	2.91 (9)	2.95 (10)	2.99
H-S(*a*)	2.95 (9)	2.94 (6)	2.90 (8)	2.88 (8)	2.89 (8)	3.00 (9)	2.96
H-S(*a*′)	3.60 (19)	3.55 (16)	3.34 (18)	3.26 (18)	3.49 (18)	3.66 (20)	3.58
H-S(*b*)	2.89 (5)	2.90 (4)	2.90 (5)	2.90 (5)	2.89 (5)	2.89 (6)	2.89
H-S(*b*′)	2.82 (2)	2.82 (2)	2.83 (2)	2.82 (2)	2.81 (2)	2.82 (3)	2.83

[a] Data from the structure of the Et_4N^+ "salt".[35]

Table VII. Angular Distortions in the Tetraphenylphosphonium "Salts" of the $M(SC_6H_5)_4^{2-}$ Complexes

	metal							
angle	Mn[a]	Fe[a,b]	Fe[c]	Co[a]	Ni[a]	Zn[a]	Cd[a]	Fe′[a,d]
α_{av}	121.5	121.9 (6)	123.0 (5)	121.6	121.8	121.7	121.5	121.5
β_{av}	118.4	117.9 (6)	120.4 (5)	118.4	118.2	118.3	118.4	118.5
γ_{av}	110	111 (2)	111 (2)	110	109	110	109	113
δ_{av}	110	100 (1.6)	100 (1.7)	96	92	98	101	106
ϵ_{av}	117	117 (1.5)	117 (1.9)	118	121	118	117	117
ϵ'_{av}	111.4	112.4 (8)	112.1 (6)	115.1	115.9	112.6	110.5	105.8

[a] The phenyl rings in the $M(SC_6H_5)_4^{2-}$ anion were refined as rigid bodies with exact hexagonal geometry. [b] Standard deviations from the mean are representative of entire family. [c] The carbon atoms in the phenyl rings in the $Fe(SC_6H_5)_4^{2-}$ anion were refined individually with anisotropic temperature factors; in this refinement the mean value of the C-C-C angle closest to the sulfur atom is 116.5(3)°. [d] Data from the structure of the Et_4N^+ "salt".

Table VIII. Comparison of Ligand Parameters in the Structures of the $[Cu_8(Dts)_6]^{4-}$, $[Fe(Dts)_2]^{2-}$ and $[Ni(Dts)_2]^{2-}$ Complexes[a]

	$[Cu_8(Dts)_6]^{4-}$ [b]	$[Fe(Dts)_2]^{2-}$	$[Ni(Dts)_2]^{2-}$ [c]
C=O	1.210 (19)	1.203 (12)	1.222 (5)
C=S	1.707 (24)	1.688 (14)	1.691 (4)
S-S(bite)	3.922 (14)	3.543 (8)	3.257 (2)
S-C-C[d]	137.7 (8)	129.3 (10)	123.3 (3)
S-C-C[e]	129.9 (13)	137.6 (10)	144.5 (5)
C-C-C[f]	92.3 (16)	93.0 (11)	92.2 (3)
C-C-C[g]	87.6 (10)	87.0 (9)	87.9 (3)
C-C-O	135.1 (12)	136.6 (12)	138.0 (3)
O-C-C	137.2 (11)	136.3 (11)	134.2 (3)
M-S	2.247 (10)	2.389 (7)	2.212 (2) 2.234 (2)

[a] Esd's for the reported average interatomic distances and angles were computed as follows: $\sigma = [\Sigma_{i=1}^{N}(x - \bar{x})^2/(N-1)]^{1/2}$, where x_i is the length of the bond and $\bar{x}$ is the mean value for the N equivalent bond lengths. [b] From ref 20b. [c] From ref 20a. [d] Chelate ring angle. [e] Exo-chelate ring angle. [f] Central C attached to S atom. [g] Central C attached to O.

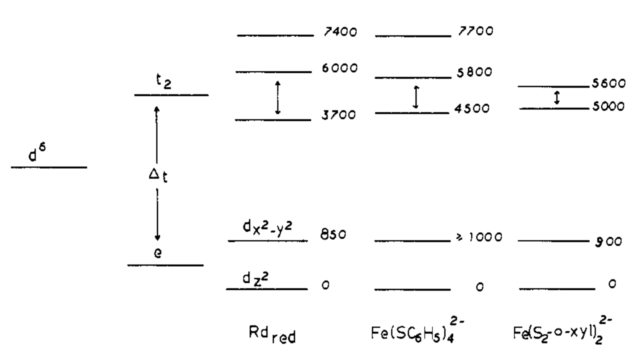

Figure 11. The ground-state electronic structure of the $Fe^{II}S_4$ tetrahedral chromophore in various ligand environments.

the electronic absorption spectra of complex I (Table X) and the values of D and E of Table IX results in a spin–orbit coupling constant, $\lambda = -95 \pm 5$ cm^{-1}, which may be compared to the ionic value for Fe^{2+}, $\lambda = -103$ cm^{-1}. A larger value of λ (-104 ± 3) is calculated for complex II, implying more ionic character for the Fe–S bonds of this complex as expected from its larger average Fe–S distance.

Table IX. Parameters of Fine and Hyperfine Structure for the $Fe^{II}S_4$ Cores in I, Rd_{red}, and II

	$Fe(SPh)_4^{2-}$	Rd_{red} [d]	$Fe(dts)_2^{2-}$
D, K	8.6[a]	10.9	9.2
E, K	2.04[a]	3.1	2.5
g_x	2.12	2.11	2.1
g_y	2.19	2.19	2.14
g_z	2.01	2.0	2.01
A_x, mm/s	1.16	1.36	1.05
A_y, mm/s	0.57	0.56	0.4
A_z, mm/s	2.09	2.03	1.6
ΔE_Q,[b] mm/s	−3.24	−3.25	−3.97
η	0.67	0.65	0.65
δ,[c] mm/s	0.66	0.70	0.668
μ_{eff}, μ_B	5.1	5.05[e]	5

[a] Taken from far-infrared magnetic resonance measurements.[44] [b] At 4.2 K. [c] At 4.2 K with respect to Fe metal at room temperature. [d] Reference 43. [e] Reference 8.

The main conclusion that may be drawn from the Mössbauer results is that the electronic structure of the active center in Rd_{red} can be accurately reproduced by the anion $[Fe(SPh)_4]^{2-}$. The anion $[Fe(dts)_2]^{2-}$ appears with a different electronic structure and cannot be considered as a suitable analogue of Rd_{red}. This difference may arise from the slightly different molecular geometry of this complex.

The $Na[Ph_4As][Fe(S_2\text{-}o\text{-xyl})_2]$ complex, which has also been suggested as a successful analogue for Rd_{red}, displays similar zero field Mössbauer spectra with hyperfine parameters and temperature variation close to those of the protein and the $[Fe(SPh)_4]^{2-}$ analogue. The magnetically perturbed spectra of this complex, however, are different from those of the protein and complex I.[19] Although a complete analysis of these spectra has not been reported, their variation with the external magnetic field indicates that the electronic structure of the ground-state spin quintet is different than that of Rd_{red} and the $[Fe(SPh)_4]^{2-}$ analogue.

Magnetization measurements were performed between 4.2 K and room temperature. Figure 12 shows the temperature variation of the magnetic susceptibility of complex I. The solid line in the figures is the result of a calculation of the magnetic susceptibility by using the electronic spin Hamiltonian (1) and the parameters listed in Table IX.

Electronic Spectra. $[Fe(SC_6H_5)_4]^{2-}$. The spectra of this complex anion were obtained in CH_3CN solution and in the solid state by

Table X. Solution and Reflectance Ligand Field Spectra of Iron(II) and Cobalt(II) Thiophenolate Complexes

complex	soln[a]	reflectance	assignt	ref
$[Fe(SC_6H_5)_4]^{2-}$	5880 (98)	5900	$^5E \rightarrow {}^5T_2$	*b*
	19 000 (sh)	7700 (sh)		
		19 530		
$[Co(SC_6H_5)_4]^{2-}$	6900 (br, 211)	6009	$^4A_2 \rightarrow {}^4T_1$ (F)	
		8333 (sh)		
	13 800 (675)	13 888		
	14 700 (820)		$^4A_2 \rightarrow {}^4T_1$ (P)	22
	16 000 (590)	22 730		
Rd_{red}	3703[c]		$^5E \rightarrow {}^5T_2$	10
	6250 (130)			
Rd_{red} (Co(II) substituted)	13 368			
	14 600		$^4A_2 \rightarrow {}^4T_1$ (P)	46
	16 130			
$[Fe(SC_6H_5)_2(Dts)]^{2-}$	5880 (95)	6040	$^5E \rightarrow {}^5T_2$	22
		19 160		
$[Co(SC_6H_5)_2(Dts)]^{2-}$	6900 (sh)	6756	$^4A_2 \rightarrow {}^4T_1$ (F)	22
	8200 (154)	8333 (sh)		
	141 80 (1080)	13 297		
	150 80 (1214)	14 705	$^4A_2 \rightarrow {}^4T_1$ (f)	
	172 40 (846)	16 666		
$[Fe(Dts)_2]^{2-}$	5800 (41)	4800	$^5E \rightarrow {}^5T_2$	20, *b*
		5550		
$[Co(Dts)_2]^{2-}$	8300 (136)	8300	$^4A_2 \rightarrow {}^4T_1$ (F)	20
	151 00 (281)	147 00	$^4A_2 \rightarrow {}^4T_1$ (P)	
$[Fe(S_2\text{-}o\text{-xyl})_2]^{2-}$	5000 (109, sh)		$^5E \rightarrow {}^5T_2$	19
	5555 (123)			

[a] CH_3CN. Values expressed in nanometers with ϵ values in parentheses. [b] This work. [c] Aqueous solution (^2H_2O).

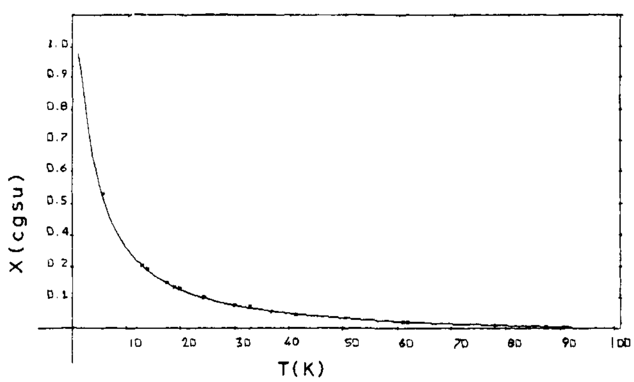

Figure 12. Temperature variation of the inverse magnetic susceptibility of the $[Fe(SPh)_4]^{2-}$ anion. The solid line represents a simulation of the data.

reflectance spectroscopy (Table X). Phenyl group absorptions in I mask the UV region of the spectrum. However, the ligand field spectra in the near-IR region show transitions that are expected to arise from the $^5E \rightarrow {}^5T_2$ transition for Fe(II) in T_d symmetry. A band at 5880 cm^{-1} (ϵ = 98), a shoulder at 7700 cm^{-1}, and the onset of an apparent transition at 5000 cm^{-1} are characteristic of an axially distorted tetrahedral ligand field.

The electronic spectra of Rd_{red} from *C. pasteurianum* have been obtained in D_2O[4a] and H_2O. Two intense charge-transfer absorptions at 333 (ϵ = 6300) and 311 nm (ϵ = 10 800) are found in the UV region of the spectrum. On the basis of electronic absorption and CD spectra analyses, bands at 6250 (ϵ = 130) and ~3700 cm^{-1} in the near-IR region of the spectrum have been assigned to the $^5E \rightarrow {}^5T_2$ transition of a Fe(II) ion in an axially distorted tetrahedral ligand field. This axial distortion which accounts for the apparent splittings of the t_2 orbitals by about 2500 cm^{-1} is apparent in the structure of the $Fe^{II}S_4$ core in Rd_{red} which appears as a flattened tetrahedron with approximate D_{2d} symmetry.[47] An examination of the distortions in the structure of I reveals a similar type of distortion. We have been unable to ascertain the magnitude of the splitting in the t_2 orbitals in I because the low-energy component of the $^5E \rightarrow {}^5T_2$ transition falls outside the range of the spectrometer. However, on the basis of the inflection present in the spectrum we place this absorption between 5000 and 4000 cm^{-1}.

The splitting of the $^5E \rightarrow {}^5T_2$ transition in I is larger than that observed for the same transition in $[Fe(S_2\text{-}o\text{-xyl})_2]^{2-}$ (Figure 11) and consistent with the larger distortions found in the structure of I.

Tha apparent similarity of the ligand environments and exact values for Δt in Rd_{red} and I cannot be established accurately because of the splittings in the t_2 orbitals. A close similarity also is evident in the ligand field spectra of the Co(II)-substituted Rd_{red}[48] and $[Co(SC_6H_5)_4]^{2-}$ (Table X). The characteristic triplets of absorption that arise from the $^4A_2 \rightarrow {}^4T_1$ (P) transitions are found at 13 368, 14 600, and 16 130 cm^{-1} and at 13 800 (ϵ 675), 14 700 (820), and 16 000 (590) cm^{-1}, respectively, for Rd_{red} (Co(II) substituted) and $[Co(SC_6H_5)_4]^{2-}$.

Summary

There is little doubt that the electronic ground state of I is close to being identical with that of Rd_{red}. The apparently different electronic characteristics of the ligand in II result in a ground state for this complex that in fine detail does not resemble Rd_{red}. The absence of $-CH_2S$ ligands in I would place this complex, by criteria suggested previously,[49] in a category of limited physiological significance. It should be emphasized however that in addition to the requirement for ligands with a terminal $-CH_2S^-$ group, a Rd_{red} active site analogue complex should also comply with the geometric characteristics of the active site in Rd_{red}. In this site, spectroscopic data suggest that the FeS_4 unit is subject to considerable distortion toward approximate D_{2d} symmetry.

A detailed structural analysis of the $[Fe(SPh)_4]^{2-}$ complex shows such an approximate distortion which apparently is a fortuitous result of intramolecular interactions. To what extent this distortion affects the ground-state electronic structure in $Fe^{II}S_4$ tetrahedral complexes is not clear; however, the magnetically perturbed Mössbauer Spectra of the $Fe(S_2\text{-}o\text{-xyl})_2{}^{2-}$ complex (in which the FeS_4 unit is not severely distorted) are different from those of Rd_{red} and I. The FeS_4 unit in the $Fe(S_2\text{-}o\text{-xyl})_2{}^{2-}$ analogue, which by virtue of the presence of $-CH_2S^-$ ligand appendices can be con-

(47) This distortion is apparent in Figure 2 and the accompanying table in ref 4a.

(48) May, S. W.; Kuo, J. Y. *Biochemistry* **1978**, *17*, 3333.
(49) Holm, R. H.; Ibers, J. A. In "Iron Sulfur Proteins"; Lovenberg, W., Ed.; Academic Press: New York, 1977; Vol. 3, Chapter 7.

sidered physiologically acceptable is closer to T_d symmetry than the FeS_4 unit in I.

Acknowledgment. The financial support of this project by a grant (No. 1R01GM18144-01A1) from the U.S. Public Health Service (D.C.) is gratefully acknowledged. We also thank Dr. V. Petrouleas for numerous fruitful discussions on the Mössbauer and magnetic susceptibility aspects of this work. D.C., A.S., and A.K. acknowledge the partial support of this work from a grant administered through the Scientific Affairs Division of N.A.T.O.

Supplementary Material Available: Listings of observed and calculated structure factors for compounds I and II (39 pages). Ordering information is given on any current masthead page.

Generation of Rhodium(II) and Rhodium(I) from the One-Electron Reduction of Tris(2,2′-bipyridine)rhodium(III) Ion in Aqueous Solution[1]

Quinto G. Mulazzani,*[2a] Silvano Emmi,[2a] Morton Z. Hoffman,*[2b] and Margherita Venturi[2c]

Contribution from the Istituto di Fotochimica e Radiazioni d'Alta Energia, Consiglio Nazionale Delle Ricerche, 40126 Bologna, Italy, and Department of Chemistry, Boston University, Boston, Massachusetts 02215. *Received September 8, 1980*

Abstract: The reaction of $Rh(bpy)_3^{3+}$ with radiation-generated reducing radicals (e_{aq}^-, $\cdot CO_2^-$, and $(CH_3)_2\dot{C}OH$) in aqueous solution quantitatively and rapidly ($k = 10^9$–10^{10} M^{-1} s^{-1}) yields $Rh(bpy)_3^{2+}$ (λ_{max} 485 nm, ϵ_{max} 1.0×10^3 M^{-1} cm^{-1}) which undergoes slow ($k = 0.45 \pm 0.05$ s^{-1} at pH 3–10) loss of bpy at room temperature. $Rh(bpy)_3^{2+}$ reacts with O_2 ($k = 4.9 \times 10^8$ M^{-1} s^{-1}) via electron transfer. In alkaline solution, $Rh(bpy)_3^{2+}$ undergoes disproportionation with ligand-labilized Rh(II) to form $Rh(bpy)_3^{3+}$ and red-violet $Rh(bpy)_2^+$. At pH >10, ligand-labilized Rh(II) reduces $Rh(bpy)_3^{3+}$ resulting in a redox-catalyzed ligand-labilization chain reaction; at pH 14, $G(bpy) \simeq G(-Rh(bpy)_3^{3+}) > 300$. The nature of O_2-sensitive $Rh(bpy)_2^+$, its spectrum, and state of aggregation is highly dependent upon the pH of the solution, [Rh(I)], and the nature and concentration of the counteranion. At least four forms of $Rh(bpy)_2^+$ are clearly identified: (a) a red-violet soluble form (λ_{max} 518 nm, ϵ_{max} 9500 M^{-1} cm^{-1}) which is formulated as $Rh(bpy)_2(OH)_n^{(1-n)}$ and may be dimeric via hydroxide bridging (in neutral solution, very small changes in pH have a large effect on the spectrum which shows a main band at ~415 nm and a well-defined shoulder in the 470-nm region); (b) a violet insoluble form represented as $Rh(bpy)_2X$ where $X = Cl^-$, ClO_4^-, etc.; (c) a transient green form observed when the red-violet form is acidified which is formulated as $Rh(bpy)_2(OH_2)_n^+$; (d) a colorless form in acidic solution which is assigned as a hydride in which the metal center is formally Rh(III), e.g., $RhH(bpy)_2^{2+}$. At "natural" pH, H_2 is produced with an efficiency of ~25% in the absence of any catalyst. The relevance of these results to solar energy conversion schemes is examined.

Introduction

Recent studies[3,4] of the excited-state electron-transfer reaction of $*Ru(bpy)_3^{2+}$ with $Rh^{III}(bpy)_3^{3+}$ (bpy = 2,2′-bipyridine) have shown that H_2 is generated from the reduction of H_2O through the intermediacy of $Rh^{II}(bpy)_3^{2+}$ and $Rh^{I}(bpy)_2^+$. From the point of view of photochemical conversion of solar energy, this result is very exciting; at the same time, only few detailed kinetic and mechanistic studies have been carried out.[5] Although $Rh(bpy)_2^+$ can be generated[6,7] by the direct action of aqueous BH_4^- on $Rh(bpy)_3^{3+}$, it is clear that only fast kinetics techniques can be utilized to characterize $Rh(bpy)_3^{2+}$ and the resulting Rh(II) and Rh(I) species.

Recently, in our examination[8] of the one-electron reduction of $Co^{III}(bpy)_3^{3+}$ using the radiation chemical techniques of fast kinetics pulse radiolysis and steady-state continuous radiolysis, we found that $Co^{II}(bpy)_3^{2+}$ undergoes slow ($k = 3.4$ s^{-1} at pH 0.5–10.5) ligand labilization in aqueous solution; by way of comparison, the electrochemical reduction of $Rh(bpy)_3^{3+}$ in CH_3CN solution[9] also results in ligand labilization. Because of the periodic relationship of Co and Rh, the growing interest in redox reactions arising from the excited-state reactions of Rh complexes,[10,11] and our continuing investigation of the interaction of radiation-generated free radicals with polypyridines[12] and their coordination complexes,[8,13,14] we have examined in detail the one-electron reduction of $Rh(bpy)_3^{3+}$ in aqueous solution. We report here on the behavior of $Rh(bpy)_3^{2+}$, the nature of the Rh(I) species, and the implications of these results to photochemical conversion and storage of solar energy.

Experimental Section

Materials. $Rh(bpy)_3Cl_3\cdot 5H_2O$ was prepared and purified according to literature procedures.[15] A sample of the complex, prepared according to the procedures of Crosby and Elfring,[16] was kindly provided by Dr. F. Bolletta and showed identical behavior. The ClO_4^- salt was also used in some experiments. Aqueous solutions of $Rh(bpy)_3^{3+}$ are stable in acidic, neutral, and alkaline media; no changes in the absorption spectrum

(1) Research supported in part by Consiglio Nazionale delle Ricerche and in part by the National Science Foundation through Grant No. CHE79-18013 and the U.S.-Italy Cooperative Science Program (Project P-109).
(2) (a) Istituto F.R.A.E.; (b) Boston University; (c) Istituto di Scienze Chimiche, Facoltà di Farmacia, Università di Bologna.
(3) Lehn, J.-M.; Sauvage, J.-P. *Nouv. J. Chim.* **1977**, *1*, 449.
(4) Kirch, M.; Lehn, J.-M.; Sauvage, J.-P. *Helv. Chim. Acta* **1979**, *62*, 1345.
(5) Brown, G. M.; Chan, S.-F.; Creutz, C.; Schwarz, H. A.; Sutin, N. *J. Am. Chem. Soc.* **1979**, *101*, 7638.
(6) Martin, B.; McWhinnie, W. R.; Waind, G. M. *J. Inorg. Nucl. Chem.* **1961**, *23*, 207.
(7) Venturi, M.; Mulazzani, Q. G., work in progress.
(8) Simic, M. G.; Hoffman, M. Z.; Cheney, R. P.; Mulazzani, Q. G. *J. Phys. Chem.* **1979**, *83*, 439.
(9) Kew, G.; DeArmond, K.; Hanck, K. *J. Phys. Chem.* **1974**, *78*, 727.
(10) Mann, K. R.; Lewis, N. S.; Miskowski, V. M.; Erwin, D. K.; Hammond, G. S.; Gray, H. B. *J. Am. Chem. Soc.* **1977**, *99*, 5525; Miskowski, V. M.; Nobinger, G. L.; Kliger, D. S.; Hammond, G. S.; Lewis, N. S.; Mann, K. R.; Gray, H. B. *Ibid.* **1978**, *100*, 485.
(11) Ballardini, R.; Varani, G.; Balzani, V. *J. Am. Chem. Soc.* **1980**, *102*, 1719.
(12) Mulazzani, Q. G.; Emmi, S.; Fuochi, P. G.; Venturi, M.; Hoffman, M. Z.; Simic, M. G. *J. Phys. Chem.* **1979**, *83*, 1583.
(13) Mulazzani, Q. G.; Emmi, S.; Fuochi, P. G.; Hoffman, M. Z.; Venturi, M. *J. Am. Chem. Soc.* **1978**, *100*, 981.
(14) Venturi, M.; Emmi, S.; Fuochi, P. G.; Mulazzani, Q. G. *J. Phys. Chem.* **1980**, *84*, 2160.
(15) Harris, C. M.; McKenzie, E. D. *J. Inorg. Nucl. Chem.* **1963**, *25*, 171.
(16) Crosby, G. A.; Elfring, W. H., Jr. *J. Phys. Chem.* **1976**, *80*, 2206.

0002-7863/81/1503-3362$01.25/0